CHALMERS

Safe and Reliable Switching of Reactive Capacitor Banks in Sweden's Industrial Sector.

Behaviour of trancient and harmonic currents when connecting banks of reactive power compensating elements.

B.o.S Degree project in Electrical Engineering

Maja Arnhög Sleman
Patrik Lindström

Department of Electrical Engineering
CHALMERS UNIVERSITY OF TECHNOLOGY
Gothenburg, Sweden 2025
www.chalmers.se

Degree Project 2025

Safe and Reliable Switching of Reactive Capacitor Banks in Sweden's Industrial Sector.

Behaviour of trancient and harmonic currents when connecting banks of reactive power compensating elements.

Maja Arnhög Sleman
Patrik Lindström

CHALMERS

Department of Electrical Engineering
Chalmers University of Technology
Gothenburg, Sweden 2025

Safe and Reliable Switching of Reactive Capacitor Banks in Sweden's Industrial Sector.

Behaviour of trancient and harmonic currents when connecting banks of reactive power compensating elements.

Maja Arnhög Sleman
Patrik Lindström

Supervisor: Martin Westin, ABB
Examiner: Thomas Hammarström, Chalmers University of Technology

Degree Project 2025
Department of Electrical Engineering
Chalmers University of Technology
SE-412 96 Gothenburg
Telephone +46 31 772 1000

Cover: A group of three-phase capacitor banks implemented in an outside environment for medium voltage level [1], CC BY 2.0 .

Written in LaTeX
Gothenburg 2025

Acknowledgements

We would like to give our appreciations to Martin Westin for giving us the opportunity to write our thesis at ABB and helping us with contacs within and outside of the company. It has been an exciting project with close ties to a real-world application, which we have especially appreciated. We would also like to thank our supervisor and examiner Thommas Hammarstöm. We would also like to thank Annant Narula, Peiyuan Chen, and Massimo Bongiorno for their support and for helping us gain an understanding of vital aspects of the project. Finally, we would like to thank everyone who has in any way contributed to the project or shown interest in it.

Maja Arnhög Sleman & Patrik Lindström, Gothenburg, June 2025

Safe and Reliable Switching of Reactive Capacitor Banks in Sweden's Industrial Sector.

Behaviour of trancient and harmonic currents when connecting banks of reactive power compensating elements.

Maja Arnhög Sleman
Patrik Lindström
Department of Electrical Engineering
Chalmers University of Technology

Abstract

The main scope of this project aims to evaluate methods of limiting inrush current when connecting capacitor banks to a 12.1 kV grid in an industrial environment. Traditionally, Swedish industries have connected large capacitor banks in parallel to the load for reactive power compensation, using asynchronous switching methods. However, the need of reactive power compensation is changing, due to an increase of power electronics and drive systems, requiring lesser amount of reactive power compensation but greater need of filtering. Establishing guiding parameters from accepted international standard IEC 61000-2-4 to measure the performance and behavior of different methods, was a major part of the evaluation method.
Depending on the amount of reactive power (Q) compensation and harmonic filtering needed, this report suggests different solutions for different use cases. For low frequent switching rates: A pre-insertion resistor is suitable for cases with major need of Q-compensation together with a small inrush reactor. A de-tuned filter is suitable when low amounts of Q-compensation is needed, but instead the need of filtering is large. Further, a TSC is applicable for any scenario of the above, with the additional feature of being able to switch asynchronously and more frequent than the regular synchronous/asynchronous breakers. Finally, a theoretical example of a strategy using variable resistance is also evaluated, with impressive results in limiting inrush currents during switching. Even though this is not yet typically deployed for 12.1 kV voltage levels, this is by far the most effective strategy evaluated.

Keywords: inrush current, asynchronous switching, synchronous switching, drive-systems, capacitor-bank, inrush reactor, de-tuned filter, TSC, pre-insertion resistor.

Acronyms

Below is the list of acronyms that have been used throughout this thesis listed in alphabetical order:

FFT	Fast Fourier Transform
L	Inductance C
Capacitance P	Power
PF	Power Factor
Q	Reactive Power
S	Apparent Power
SVC	Static Var Compensation
THD	Total Harmonic Distortion
TSC	Thyristor Switched Capacitor

Contents

List of Figures

List of Tables

1
Introduction

1.1 Background

In Swedish industry, reactive power compensation has traditionally been achieved using large capacitor banks connected directly to the grid at the nearest substations, without filter reactors. Large transients occur due to inrush current when a capacitor is connected in an uncontrolled way, to avoid this problem a asynchronous breaker (i.e. a breaker with a built-in physical phase shift, which switches each phase with a short time interval between them) combined with a switch-sync relay has been utilized to connect and disconnect at voltage zero crossing. Swedish industry faces a problem because neither of these components is manufactured locally anymore, and the import of the same solution is not economically feasible for medium voltage levels. Thus, a new or equivalent solution is needed. As the power consumption of the industry changes when traditional motors are replaced with frequency-controlled drive-systems the need of reactive power compensation using large capacitor banks, decreases. However, frequency-controlled drive-systems consume a non-linear current due to switching power electronics, creating high-frequency harmonics, increasing the need of harmonic filtering.

1.2 Purpose

This project will investigate behavior of inrush currents in capacitors, to find one or more suitable solutions that could replace the traditional method described above. It will also investigate how each method will affect harmonic content in the system. Further, the project intend to increase the knowledge related to reactive power compensation, power quality, filtering harmonics, and inrush currents among power system designers.

1.3 Achievements

Gain understanding of how current and harmonics behaves in a high power capacitor during connection. Provide simulation models of the typical industrial power grid topology, where different deployments can be simulated and analyzed to determine the most effective way in terms of effectiveness and size to provide safe reactive power compensation in stand-alone scenario. Ideally, this simulation model could then be extended to fit a real world scenario where it could be used to determine

the optimal solution at a specific location.

1.4 Limitations

The scope of this analysis includes a typical local industrial connection, defined as a transformation from 139 kV to 12.1 kV, with reactive power compensation implemented on the 12.1 kV side. A symmetric three-phase system is assumed throughout. Moreover, as the capacitor bank is ungrounded, multiples of three can be neglected, even with the Y-connected configuration. Do not consider a solution includning active filters.

2
Theory

The following section provides the theoretical background and explains vital concepts related to reactive power compensation, inrush current, and harmonic content. In addition, it describes the software environment, including the relevant blocks and modules, which the simulations and analysis are based on.

2.1 Software

MATLAB®, together with MATLAB® Simulink, has served as the primary platform for simulation and validation of calculations throughout this project. MATLAB provides a universal software environment with a wide range of preconfigured blocks suitable for simulating complex systems. Within Simulink, components from the Simscape Electrical™ library were used exclusively to model the electrical systems. To enhance model accuracy, the Cadence OrCAD X PSpice® platform was also utilized to a limited extent, due to its more detailed and accurate component models. However, PSpice was not used as part of the main simulation workflow, but rather as a complementary tool for model verification.

2.2 Reactive power compensation

Reactive power compensation generated by shunt capacitor is needed to reduce losses and improve the total efficiency of the system [2]. Supplying the system with reactive power also helps maintain voltage stability and ensures that minimal current is drawn from the grid by improving the power factor (PF). The PF can be defined either as the cosine of the phase angle between current and voltage or as the fraction of the apparent power that is the active power. The apparent power (S) is calculated according to Equation 2.1, the active power (P) is given by Equation 2.2, and the reactive power (Q) is described by Equation 2.3. The PF serves as an indicator of how effectively the electrical system converts apparent power into useful active power.

$$S = 3UI^* = \sqrt{(P^2 + Q^2)} \tag{2.1}$$

$$P = 3UI\cos\varphi \tag{2.2}$$

$$Q = 3UI\sin\varphi \tag{2.3}$$

2.3 Harmonic content

Power electronic converters and drive systems are inherently non-linear in nature, and therefore contribute to the generation of harmonic content within the power system [3][4]. In particular, diode bridge rectifiers draw commutated currents, which introduce significant harmonic distortion. Consequently, the ongoing transition from conventional inductive motors to electronically controlled drive systems results in an increased presence of harmonic voltages and currents in electrical networks. The total harmonic distortion (THD) is calculated according to 2.4. A high THD increases the need of filtering harmonics created by rectifiers and drive systems that leaves odd harmonics in the system. However, multiples of three are canceled out in a so called zero-sequence current in a delta connection. For this case study, multiples of three are neglected also in the Y-connected system, as the capacitor bank is ungrounded in the real-world application and only symmetrical operating conditions are assumed.

$$\mathrm{THD} = \sqrt{\sum_{h}^{n} \left(\frac{U_h}{U_1}\right)^2} \tag{2.4}$$

2.4 Inrush current

Shunt capacitors, as mentioned earlier, are the most common way to provide reactive power compensation, however, uncontrolled connection causes large transient currents [5]. The inrush current through a capacitor is proportional to the rate of voltage change, as described by Equation 2.5. These generated inrush current cause a potential risk to system components and can cause voltage fluctuations that may disturb or damage sensitive equipment, such as control systems and electronic devices. Therefore, it is essential to limit current transients in order to maintain safe and reliable operation of the power grid. Furthermore, the strength of the power grid plays a significant role in how the system responds to capacitor switching. A stronger grid, characterized by a higher short-circuit power, is capable of supplying larger transient currents without experiencing severe voltage deviations.

$$i_C = C\frac{du(t)}{dt} \tag{2.5}$$

To minimize current transients, it is essential to ensure that the voltage across the capacitor is equal to the voltage at the connection bus at the moment of switching [6]. Figure 2.1 illustrates the concept and the relation between peak current and n. Equation 2.6 describes n as the square root of the ratio between X_C and X_L. When $V_{C0} = V$, i.e. when the voltage across the capacitor is equal to the bus voltage, the peak inrush current decreases as n increases. Conversely, in the two extreme cases where the ratio is either 0 or 2 the peak inrush current increases significantly with higher values of n.

$$n = \frac{1}{\sqrt{\omega^2 LC}} = \sqrt{\frac{X_C}{X_L}} \tag{2.6}$$

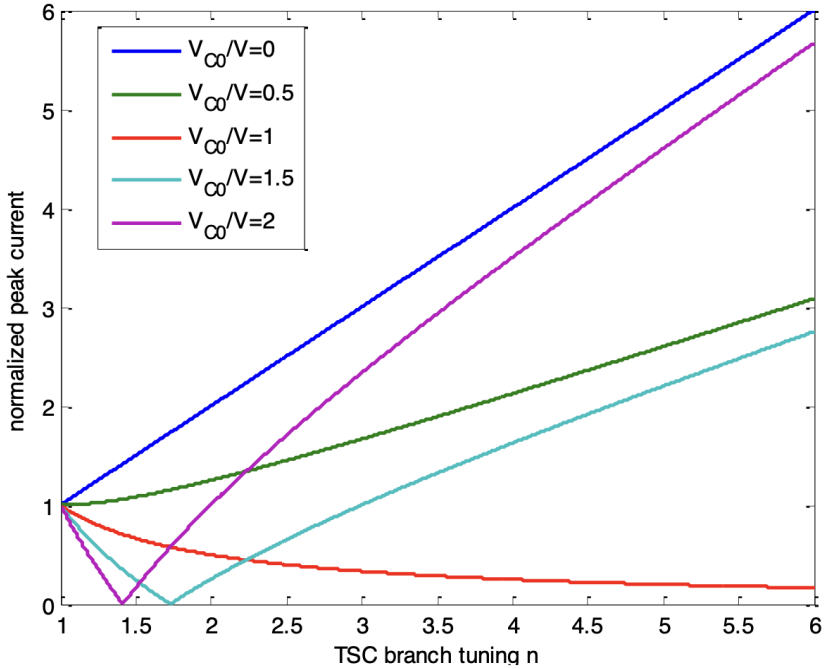

Figure 2.1: Transient currents during connection, at different voltage levels. [6]. Reprinted with permission.

An illustrative example is provided below to validate the theoretical prediction that the instant of connection significantly affects the transient behavior, illustrated by Figures 2.2-2.5. Assuming a fixed relation between X_L and X_C, it is clear that the voltage transient drastically reduces as the connection happens when the voltage of the bus is equal to the voltage across the capacitor. In the case where there is a mismatch of these voltages, an aggressive inrush of current is apparent, clearly shown in Figure 2.4. Further, there is a difference between the cases where the voltages is equal, but at different levels, e.g. when the capacitor is pre-charged or not charged. In Figure 2.5, where the capacitor is initially charged to a value at maximum or close to it, connection at this moment causes the lowest amount of transient voltage and oscillations in the system.

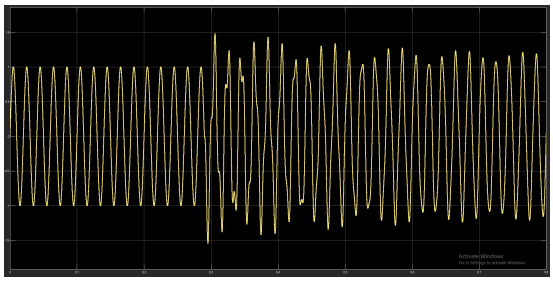

Figure 2.2: Bus voltage: $0p.u.$, capacitor voltage: $0p.u.$, giving a voltage difference $\Delta = 0p.u.$ between bus and capacitor. Transient voltage is detected, but not at extreme levels.

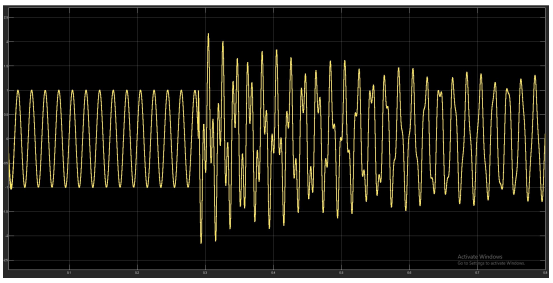

Figure 2.3: Bus voltage: $0p.u.$, capacitor voltage: $1p.u.$, giving a voltage difference $\Delta = 1p.u.$ between bus and capacitor. Significant transient voltage is detected, at twice the amplitude of the fundamental.

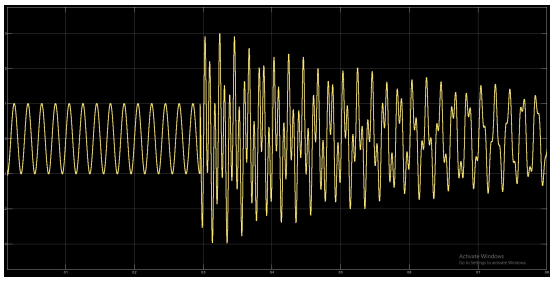

Figure 2.4: Bus voltage: $-1p.u.$, capacitor voltage: $1p.u.$, giving a voltage difference $\Delta = 2p.u.$ between bus and capacitor. Extreme transient is detected at several times the fundamental amplitude.

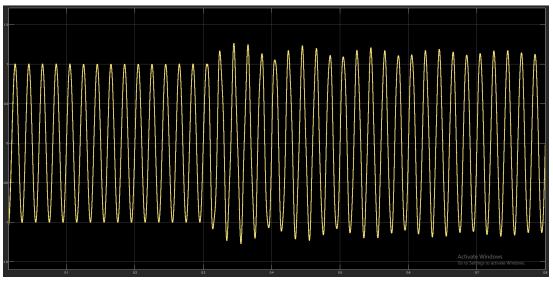

Figure 2.5: Bus voltage: $1p.u.$, capacitor voltage: $1p.u.$, giving a voltage difference $\Delta = 0p.u.$ between bus and capacitor. Almost no transient is detected, and oscillations stay close to the fundamental frequency.

2.5 Methods to restrain inrush currents and reduce harmonic content

The following sections will describe different strategy's to mainly restrain inrush currents. Some strategy's will also intend to provide filtering as an expanded replacement of the asynchronous switch and switch-sync relay.

2.5.1 Inrush reactor

Placing a relatively small reactor in series with the capacitor bank, see Figure 2.6, can help reduce current transients slightly [5]. This phenomenon is described by Equation 2.7, where the voltage is proportional to the rate of change of current. This means that the reactor is current stiff, as it inherently resists rapid changes in current. This method would help to dampen current transients, while it does not provide any significant filtering benefit to the power system. However, it introduces a resonant frequency that must be taken into account. Inrush reactors are common

to find attached to the capacitor banks regardless of connection strategy with a reactance value of 50 µH to 100 µH and is so small in size that it can physically be fitted inside the construction casing of a capacitor bank [7].

$$u(t) = L\frac{di(t)}{dt} => \frac{1}{L}\int U_L\,dt = i(t) \tag{2.7}$$

The current, $i(t)$, is the current that passes through the inrush reactor to the capacitor bank. An increase in L will decrease the fraction $\frac{1}{L}$, thus making the current $i(t)$ passing through the reactor smaller. However, increasing the size of the reactance brings challenges, it reduces the amount of reactive power compensation and the physical size of the reactor also increase significantly. Equation 2.8 governs the parameters of the reactor in relevance to it's size [8]. Though, it does not provide exact dimensions of a real-world reactor due to casing and mounting structures needed to deploy it at an industry. It does provide an insight of the minimal required size to achieve a certain reactive capability using an air gaped shunt reactor.

$$L = \frac{\mu_0 N^2 A}{l} \tag{2.8}$$

- L = inductance (henry, H)
- μ_0 = permeability of free space ($4\pi \times 10^{-7}$ H/m)
- N = number of turns
- A = cross-sectional area (m^2)
- l = length (m)

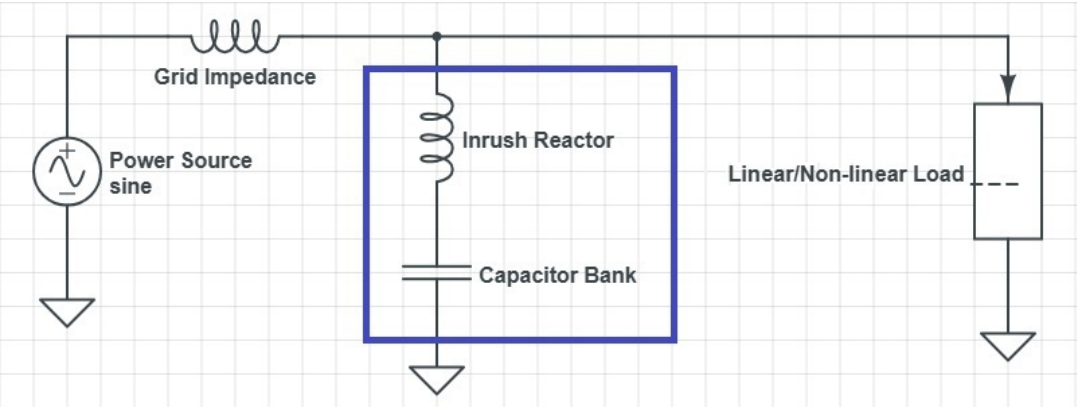

Figure 2.6: Schematic of series reactor acting as inrush reactor and/or detuned filter.

2.5.2 Pre-insertion resistor

A pre-insertion charging resistor can be used to gradually magnetize the capacitor bank. By initially placing a resistor in series with the capacitor bank, the inrush current is limited [9][10]. Limiting the current also reduces the rate of voltage change across the capacitor in relation to Equation 2.5. This pre-charging can be achieved in two ways. One method uses a fixed resistor along with two breakers to allow a controlled initial charge, as illustrated in Figure 2.7. Alternatively, a variable resistor

can be used to achieve gradual pre-magnetization with only a single breaker. This configuration, shown in Figure 2.8, allows the charging rate to be controlled by adjusting the resistance, offering the advantage of reduced switching complexity.

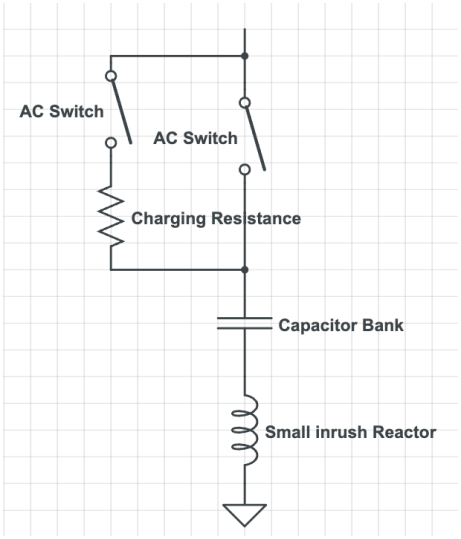

Figure 2.7: Example schematic of a fixed pre-insertion resistor.

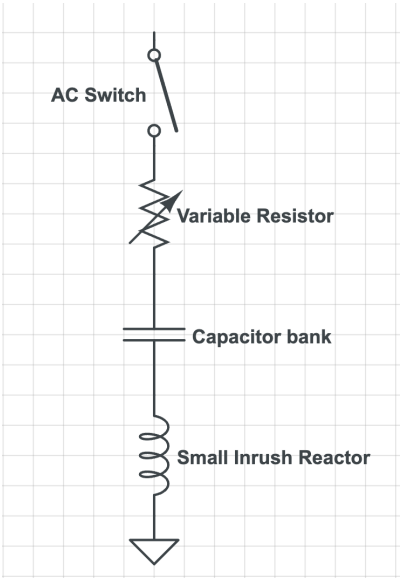

Figure 2.8: Schematic of variable pre-insertion resistor.

2.5.3 De-tuned filter

As mentioned in Section 2.5.1 above a series reactor could help limiting the surge current. Placing a larger reactor in series with the capacitor bank would serve the same purpose as the previous inrush reactor, but could also help suppressing present harmonics in the system [5]. Acting as a de-tuned filter, it would resonate at a frequency specifically chosen to be outside the problematic area of resonance — for example, at a frequency not matching the fifth, seventh, or eleventh harmonic of the fundamental, but typically below this range of frequencies. Equation 2.9 describes the resonant frequency between inductance and capacitance in the system.

$$f = \frac{1}{2\pi\sqrt{LC}} \tag{2.9}$$

Equation 2.7 describes that a reactor with large inductance value would suppress the inrush current, $i(t)$, more than the regular inrush reactor would. The main theoretic basis of the de-tuned filter is to increase it's size to a point where there is a significant reactive exchange between a capacitance an the inductive reactor, where the resonance frequency is tuned to be between odd number of harmonics and outside the problematic area as mentioned above. An example of this is shown in Figure 2.9.

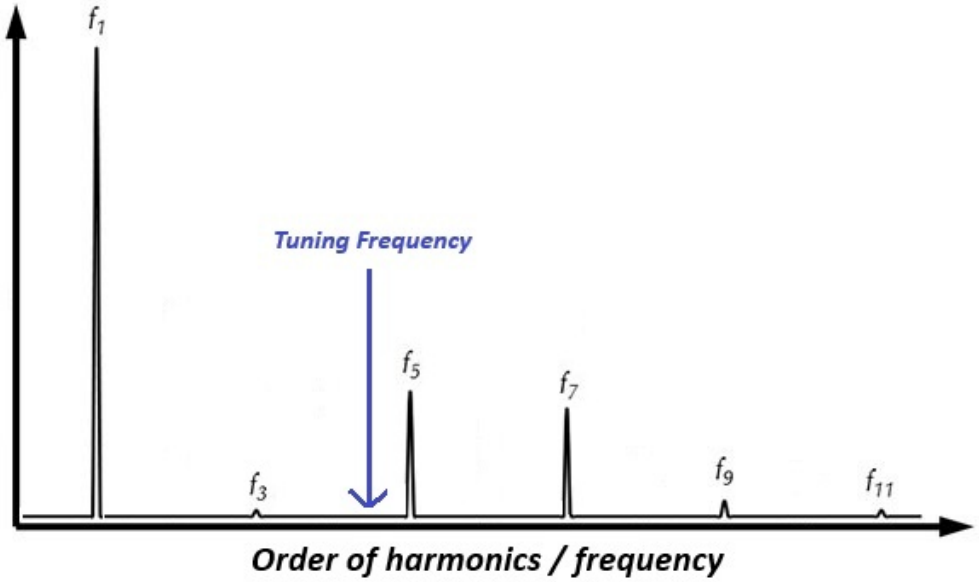

Figure 2.9: An example of placement of the tuning frequency of a de-tuned filter.

2.5.4 Thyristor-switched capacitor banks

Thyristors can be used to switch in and out the capacitor bank, the method is called thyristor switched capacitor (TSC) and would in theory lead to transient free switching, this is however impossible in the reality [6]. The equivalent single phase circuit is illustrated by 2.10, where T_1 leads positive half cycle and T_2 leads negative half cycle, the inductor is needed to limit the current during switching. The switching can be performed according to two strategy´s, A and B. In strategy A $U_C \leq \hat{U}$ and $U_C = U \cdot \sin\alpha$, where α is the phase angle of the voltage at the moment of switching. This condition will ensure the peak current to never exceed the steady state current, the behavior of different ratios between buss voltage and capacitor voltage is illustrated by Figure 2.11. If switching is performed when $U_c > \hat{U}$, switching is preformed according to strategy B, $\sin\alpha = 1$, i.e. at the maximum of the bus voltage. This strategy can lead to alarming high current transients as Figure 2.1 illustrates, again it depends on the TSC tuning n.

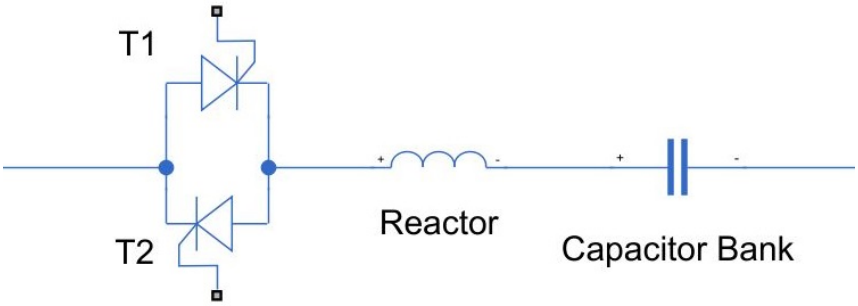

Figure 2.10: One phase equivalent of a TSC.

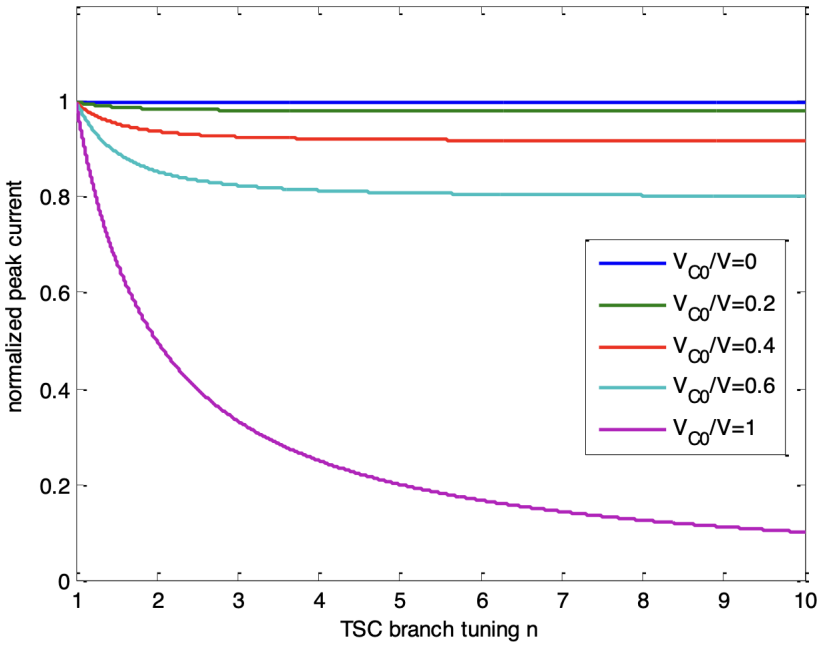

Figure 2.11: Transient current of the TSC using Strategy A [6]. Reprinted with permission.

3
Method

This chapter describes the modeling approach used in the simulation and outlines how the results are evaluated in Section 5. The chapter starts with an overview of the relevant international standard, followed by a detailed description of the MATLAB blocks and their configurations. Finally, the chapter presents each individual limitation methods and their specific implementations to limit inrush current.

3.1 International standards and conventions

According to Swedish Institute for Standards there are international standards used to regulate the containment of voltage fluctuations and voltage transients in industry environments that occur due to switching mechanisms [11]. SS-EN 50160 regulate the accepted behavior of public networks, while IEC 61000-2-4 regulate the behavior of non-public industrial networks. Since reactive power compensating elements in industrial environments are being evaluated in a non-public setting, IEC 61000-2-4 will be used to establish a reference of tolerated magnitudes. It should be mentioned that either of these standards does not provide any or numerical guidelines regarding tolerances of transient behavior and magnitudes, other than referring to the manufactures guidelines of the specific equipment being used in each respective use case. This is problematic since transient behavior is the main scope of this analysis, therefor requiring certain estimations to be made for evaluating the results of different inrush current limiting methods. This will be further explained in Section 3.1.1. The allowed amount of disturbance is dependent on what classification the facility has [11]. The different classes contain various equipment that all have different protection levels or sensitivity for disturbances where class 1 have the highest sensitivity level, class 2a, 2b and 2L is in the middle and class 3 have the hightest tolerance level.

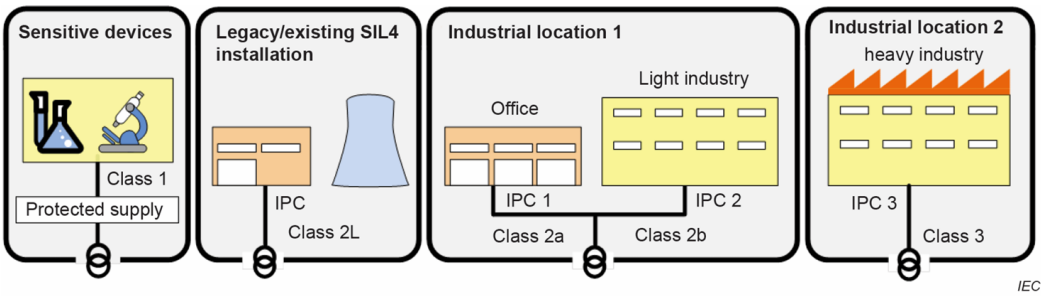

Figure 3.1: Explanation of classes included in IEC 61000-2-4 [11]. Reprinted with permission.

3.1.1 Transient impact evaluation method

The international standard IEC 61000-2-4 does not parametrically provide insight of tolerated magnitudes of transients. However, it does provide an numerical example of a tolerance envelope for IT/sensitive equipment, which fall under the sensitive class 1 category. Class 1 equipment is the most sensitive kind and cannot handle any larger long lasting transients. Therefore, assumption will be made that sensitive class 1 equipment is used, since this highest level of voltage quality is acceptable for all other types of equipment classes. It is also a relevant assumption to make due to the fact that older industrial machinery gets replaced by newer machinery operated by drive systems and more advanced control systems. These computer based systems rely heavily on proper power system quality with little to no voltage fluctuations to function properly without introducing accelerated aging.

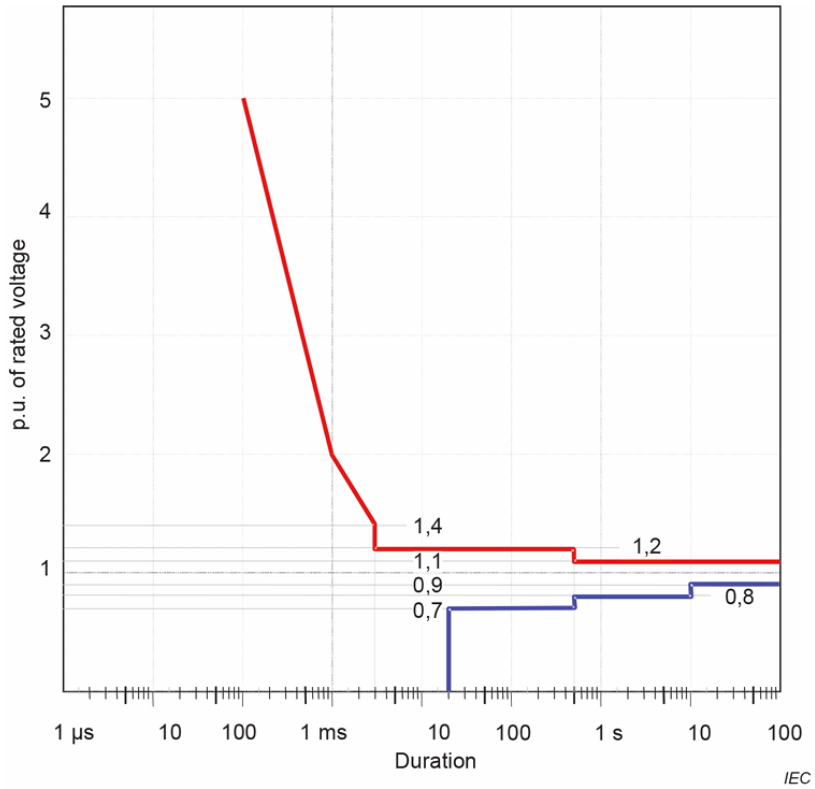

Figure 3.2: Illustration of allowed transient phenomena for IT equipment as specified in IEC 61000-2-4 [11]. Reprinted with permission.

3.1.2 Harmonic content evaluation

The international standard IEC 61000-2-4 provides regulation regarding THD, calculated according to Equation 3.1 [11]. The summation is taken from $h = 2$ to $h = 40$, covering the 2nd to the 40th harmonic. For class 1 a THD of 5% is considered an acceptable amount, further the standard presents a table specifying a percentage for each individual harmonic, for example is 2% allowed for $h = 2$, 3% for $h = 3$, 1% for $h = 4$ and 3% for $h = 5$ and so forth.

$$\mathrm{THD} = \sqrt{\sum_{h=2}^{40} \left(\frac{Q_h}{Q_1} \right)^2} \tag{3.1}$$

where:

- Q_1 is the RMS value of the fundamental frequency component
- Q_h is the RMS value of the h-th harmonic component

3.2 Blocks in the Basic simulation model

The basic simulation model contains a simulated regional grid of 139 kV connected via a transformer to a local grid of 12.1 kV. The capacitor bank is connected via a breaker at the local grid. Parameter values in the following blocks were chosen to

simulate a typical industry in the Swedish infrastructure and some assumption has been made to complete the model. Assumed parameters has been cross referenced with typical industries on-site actual data.

3.2.1 Thevenin equivalent

An ideal three-phase voltage source behind an impedance was used to model the grid, shown in Figure 3.3. The voltage source had a phase-to-phase voltage of 139 kV and 50 Hz. It was connected in Yg, meaning that all three sources were connected in Y configuration to an internal grounded neutral. It was configured with load flow set to swing, as it was used as the only source in the model. The swing bus compensated for any mismatch between the total generated power and the total load [12]. The line impedance was modeled by usage of values from the use case, where the nominal voltage was 139 kV and the short circuit current was 19.54 kA. Further the $\frac{X}{R}$ ratio was assumed to be 10. Using Equation 3.2 the total line impedance could calculated to approximately 4.11 Ω. Resulting in a line inductance of 0.013 H and a line resistance of 0.41 Ω.

$$Z = \frac{U_n}{\sqrt{3} I_k} \tag{3.2}$$

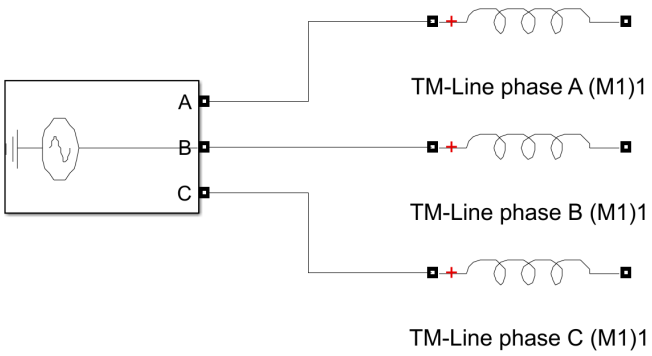

Figure 3.3: Three-phase voltage source modeled as a Thevenin equivalent.

3.2.2 Transformer

A non-ideal three-phase transformer of 139 kV/12.1 kV was used to simulate the transformation of voltage from the regional grid to the local grid. The transformer had a nominal power of 100 MV A and was set to operate at 50 Hz. The nominal power can be considered relatively high for this case, a lower rated power level would lead to higher internal resistance and inductance, in MATLAB these values increase proportionally, causing the same $\frac{X}{R}$-ratio. Changing the rated power, however, causes the resonant frequency to change, a higher intrnal inductance will lead to a lower tuning frequency. The internal resistance and inductance as well as the magnetization resistor and magnetization inductance are given in Table 3.1. Further, the transformer connections was configured using Yg/Yn, in this way the

primary side and the secondary side had proper and independent grounding, which is crucial for fault detection and safe operation [13]. To simulate different grid impedance's and how it affects the sensitivity of the system, four scenarios have been conducted using identical models of the transformer; single transformer, two parallel transformers, three parallel connected transformers and finally four parallel connected transformers.

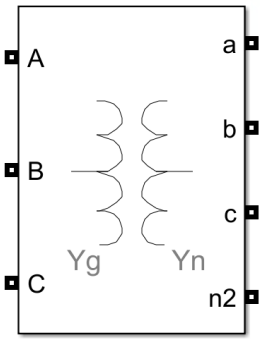

Figure 3.4: Three-phase transformer block.

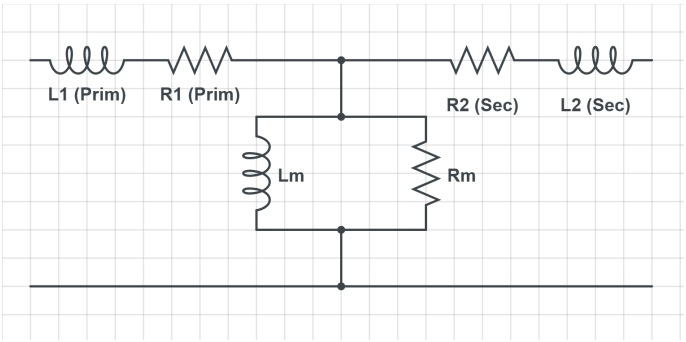

Figure 3.5: Transformer equivalent circuit with leakage inductance's, winding resistances and magnitixing branch.

Table 3.1: Transformer parameter values in p.u.

Parameter	p.u. value
Internal resistance (R1&R2)	0.002
Internal inductance (L1&L2)	0.08
Magnetization resistance (Rm)	500
Magnetization inductance (Lm)	500

3.2.3 Capacitor bank configuration

The three-phase series RLC-Branch block was used to model the capacitor bank [14], as illustrated in Figure 3.6. Resistance and inductance were excluded. The capacitance value was varied in a range from 2 MVAr to 20 MVAr in 10 steps. In this way, the behavior of inrush current, voltage oscillations and time to steady state could be analyzed for different sizes of capacitor banks.

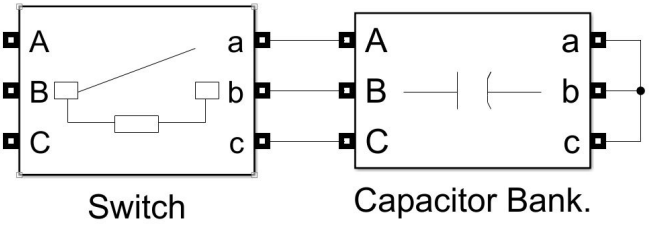

Figure 3.6: Configuration of capacitor band including a three-phase switch.

The capacitor bank was connected through a three-phase breaker, it was set to close at t =0.063 33 µs, i.e. when phase A was at it´s peak value, simulating worst case scenario [5]. The capacitance values were calculated using Equation 3.3 - 3.5, by determining the current from the actual reactive power of each case.

$$I = \frac{Q}{\sqrt{3}U} \tag{3.3}$$

$$X_c = \frac{U}{I} \tag{3.4}$$

$$C = \frac{1}{2\pi f X_c} \tag{3.5}$$

3.2.4 Functions to extract measurements

To find the extreme values of current and voltage as well as time to steady state the C/C++ block was integrated [15]. The source code for each block can be found in Appendix A.

The functions for determining the maximum values in both current and voltage measurements were designed to continuously compare each new measured value with the currently stored maximum. If the new value was greater, it replaced the previous maximum.

The function to find time to acceptable voltage level (time to steady state) was designed to measure the time by starting the clock when closing the switch and stop the clock when all three phases were below the maximum limit. According to [11] the allowed voltage deviation for class 1 is ±8% of the nominal voltage or 0.08 in the per unit system. Steady state was defined as an acceptable voltage level for 1000 samples, i.e. 2.5 ms, meaning being within the interval of [0.92, 1.08] p.u..

3.2.5 Non-linear loading

To evaluate the impact of various methods on the system's harmonic content, a nonlinear load was introduced to emulate the widespread of different loading types at a typical industry. A simplified schematic is shown in Figure 3.7, consisting of four types of loads in total. Load A and C was set to be constant impedance load, while load B and D was set to be a constant power load. These are combined in parallel with a Universal Bridge, configured as a diode bridge for AC/DC conversion, followed by an inverter controlled by a triggering signal to convert DC back to AC. The composition of the linked rectifier and inverter will emulate the harmonic behavior of a typical drive-system. This configuration allows the pulse-width modulated bridge to simultaneously switch loads C and D, thereby creating a worst-case scenario in terms of harmonic distortion amplitudes.

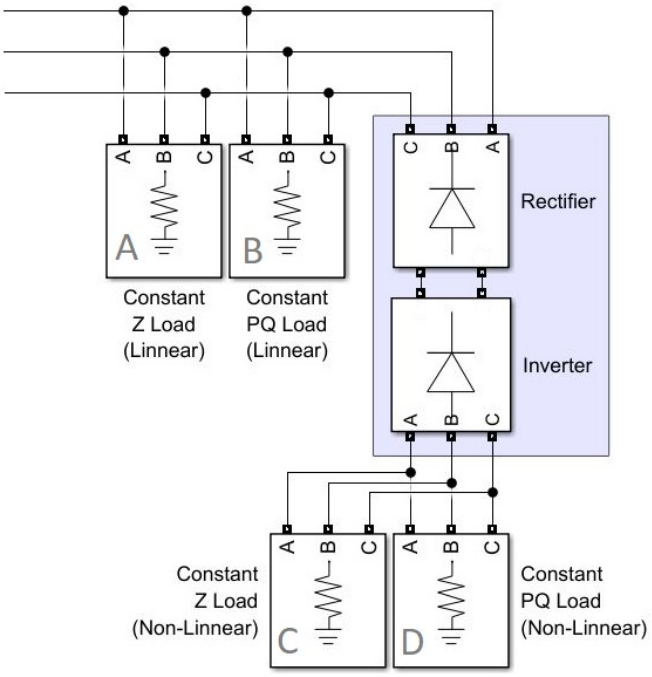

Figure 3.7: Simplified scematic of linear- and non-linear load

3.3 Methods to restrain inrush currents and reduce harmonic content

All of the following methods were based on the basic simulation model described in Section 3.2. The different methods to limit inrush current and possibly reduce harmonic content will be described in the following sections and the results of each method are presented in Section 5. All simulations of limitation methods are based on a compensation of 8 MVAr capacitive reactive compensation and a grid consisting of only one transformer.

3.3.1 Inrush reactor

The inrush reactor was modeled as a three phase RLC branch where R and C was excluded [14]. To determine the required inductance value for sufficient current limitation while staying within the constraints described in Section 3.1, various reactor sizes were evaluated. The reactor was connected in series after the switch, as shown in Figure 3.8. The results are presented in Section 5.2.1.

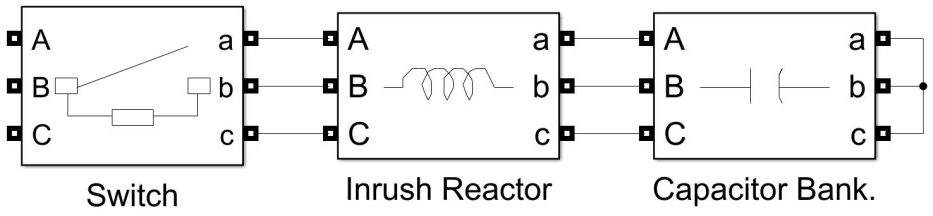

Figure 3.8: Simulation setup for inrush current analysis, showing the switch, series-connected inrush reactor, and capacitor bank.

3.3.2 Pre-insertion resistor

Two different strategies using a pre-insertion resistor were evaluated. Case 1 was modeled as in Figure 3.9 and Case 2 were modeled as illustrated in Figure 3.10. In Case 1, Breaker 1 closes first at $t = 0.0633s$, followed by Breaker 2 at $t = 0.2995s$. To determine a suitable value for the pre-insertion resistor, repeated simulations were conducted, and the best-performing configuration is presented in Section 5.2.2. Case 2 uses the resistor differently: the resistance starts at a high value and linearly decreases over time, from $100\,\Omega$ to $0\,\Omega$. The variable resistance was electronically controlled by a function block combined with a time block in the simulation.

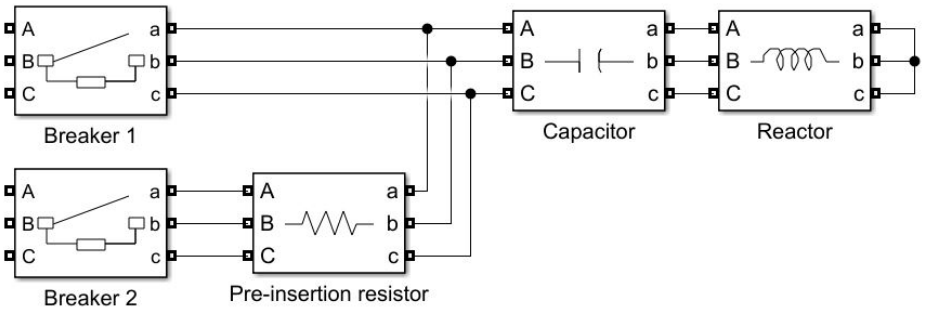

Figure 3.9: Simulation model for Case 1 using a pre-insertion resistor, where Breaker 1 closes before Breaker 2 to limit inrush current during capacitor magnetization.

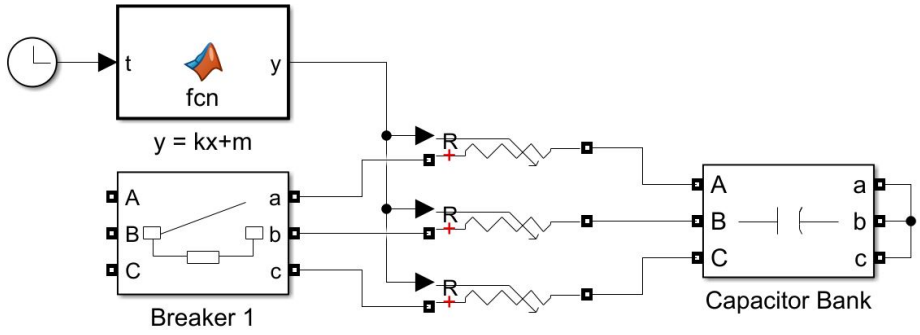

Figure 3.10: Simulation model for Case 2 using a variable pre-insertion resistor, utilizing only one breaker.

3.3.3 De-tuned filter

Two cases of de-tuned filters were evaluated, specified parameters are presented in Table 3.2. Case 1 was a de-tuned filter, which placed the tuning frequency at 4.7 times the fundamental, i.e., 235 Hz. Case 2 was tuned to the 4th harmonic, i.e., 200 Hz. The total inductance of the transmission line and transformer at the secondary side was calculated to be approximately L_{grid} =0.844 mH, by usage of Equation 3.6. The required inductance for each case was calculated using Equation 3.7 by solving for L_{filter}. The inductance value for Case 1 was found to be approximately 1.793 mH, and 2.687 mH for Case 2. These values were implemented in the simulation in the same configuration as the inrush reactor (see Figure 3.8). Furthermore, an FFT analysis was performed to assess harmonic suppression. The results of inrush current limitation and harmonic mitigation are presented in Section 5.2.3.

$$Z_{sec} = Zprim(\frac{Usec}{Uprim})^2 \tag{3.6}$$

$$f = \frac{1}{2\pi\sqrt{(L_{grid} + L_{filter})C}} \tag{3.7}$$

	Frequency (Hz)	Harmonic	L_{filter} (mH)	L_{grid} (mH)	L_{tot} (mH)
Case 1	235	4.7	1.793	0.844	2.637
Case 2	200	4	2.687	0.844	3.531

Table 3.2: Tuning frequency's and associated inductance values.

3.3.4 Thyristor-switched capacitor

An ideal TSC was implemented in the base simulation model. It included six thyristors in total, two assigned to each phase, along with a simplified trigger system. The thyristors were configured to conduct by a Delay On block to control each phase separately. Two cases were evaluated, both cases conducted the thyristors in order to match the voltage levels, ($V_{C0} = V_{bus}$), as the single-phase example in Section 2.4

clearly demonstrated that this condition results in the lowest voltage fluctuations. In Case 1, each phase was triggered during three immediately successive oscillation cycles, separated by $t = 6.67ms$ corresponding to a 120° phase shift. In Case 2, a hold time was introduced between each trigger signal, with the objective of spreading out the switching events and reducing the amplitude of the resulting voltage oscillations.

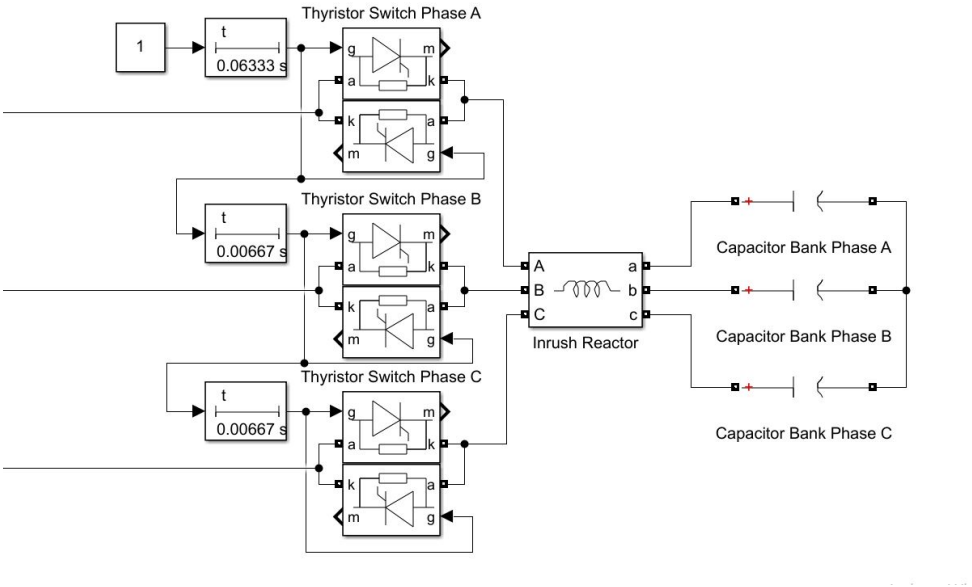

Figure 3.11: Simulation model emulating a three-phase TSC switching mechanism with a small inrush reactor.

4

Implementation

This section will describe the method used to study the behavior when closing the capacitor bank. The first section will describe the schematic of the basic simulation model, without any sort of inrush current limitation method. Followed by sections describing different strategies to limit current transients and/or suppress or eliminate harmonics. All measurements are in per unit definition.

4.1 Basic simulation model schematic

A simplified schematic of the basic simulation model is shown in Figure 4.1, the full version can be found in appendix A.

Blocks described in Section 3.2 combined with measurement blocks constitutes the complete model. Measurements of current and voltage were continuously performed at points A B and C. The grid was modeled as a Thevenin equivalent to give better flexibility and allowing measurement of the fundamental signal. At point C, the current was analyzed trough a C/C++ -function to find the max value of the current transient. This value was exported to an array in the MATLAB file where it´s value was extracted. Further, voltage measurements of each phase were conducted to perform mathematical operations, the fundamental signal of each phase were subtracted from the total signal at point C, allowing analyze of only the oscillations at point D.

To find the max value of the voltage deviation transient, a C/C++ -function were utilized and exported to the same array as the current value. The oscillations were also put through a C/C++-function to find the time elapsed from closing the switch to when the signal reach steady state.

To simulate the connection behavior without any form of current limitation, a series of simulations using a three-phase breaker were performed for various capacitor bank sizes. In order to analyze the impact of grid impedance on peak current and voltage deviation, the simulations were repeated for different grid strengths by modeling one, two, three, and four transformers connected in parallel. The results are presented in Section 5.1.

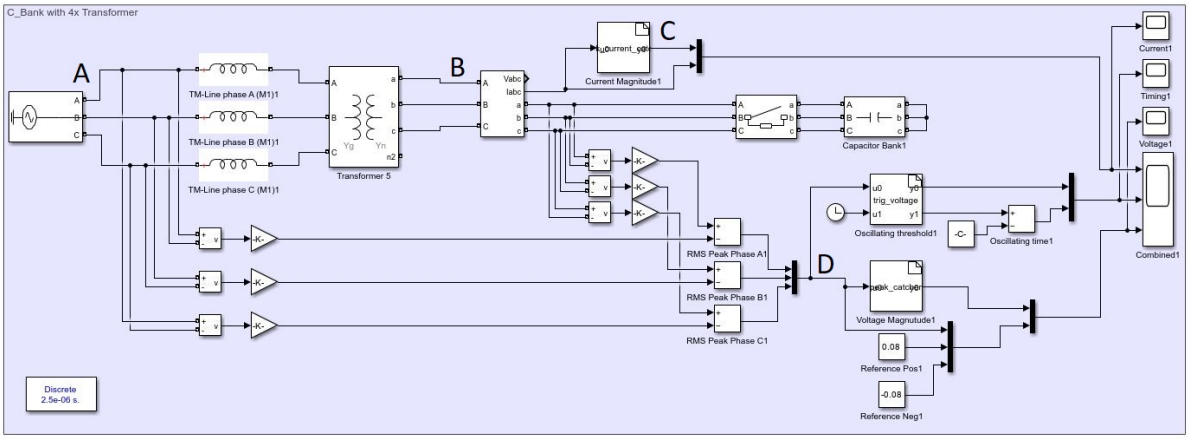

Figure 4.1: Simulation model of the base scenario, including transformer setup, current and voltage measurement points (A–D), and signal processing for transient and steady-state analysis.

4.1.1 Non-linear loading

The total load consists of a mixture between linear and non-linear loads as well as a mixture of constant power loads and constant impedance loads. Measurements to conduct a FFT of the voltage is performed right after the transformer, at point B in 4.1. The FFT was preformed via a Simout block and exported to the MATLAB file to find the THD and visualize a frequency spectrum.

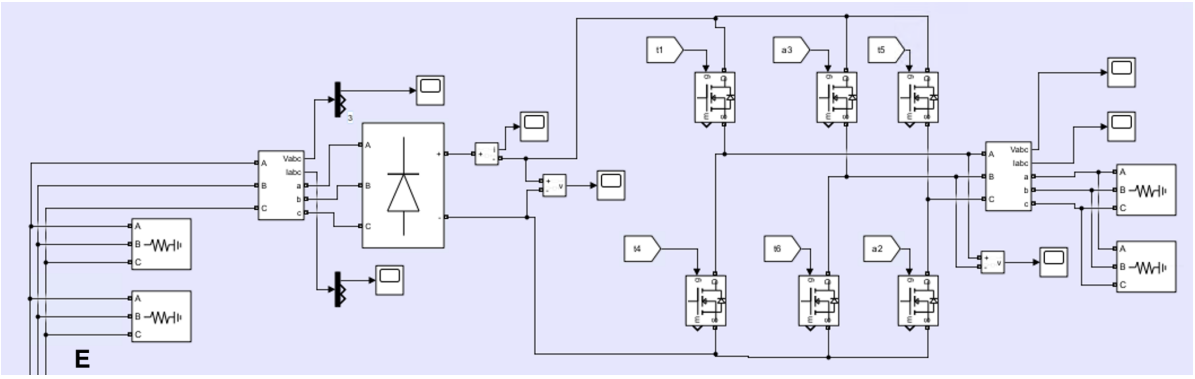

Figure 4.2: Simulation model of the non-linear load.

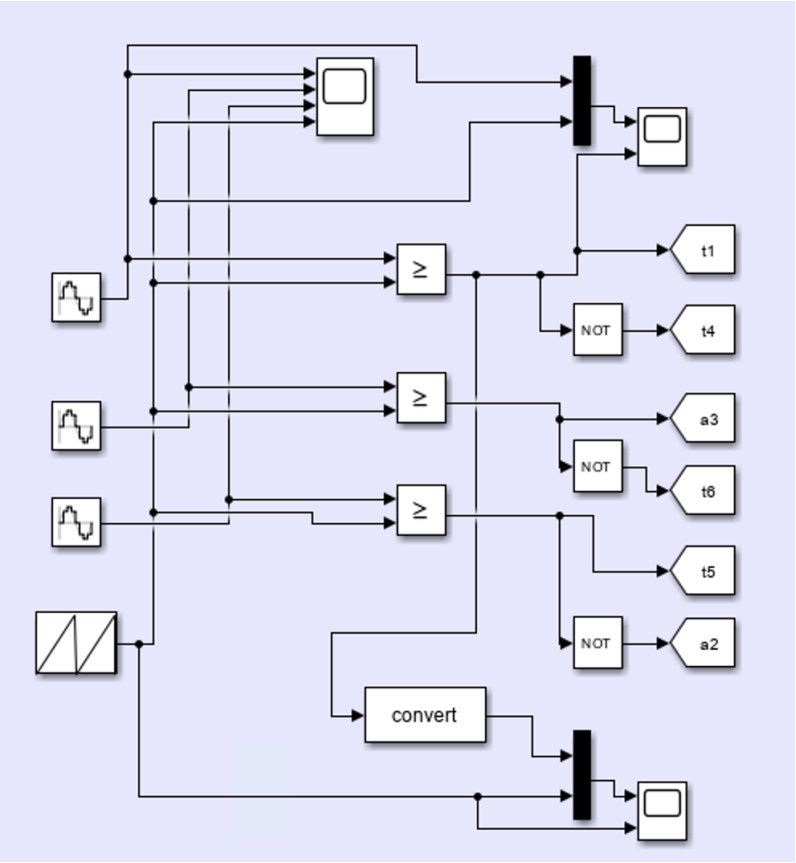

Figure 4.3: Control circuit for the non-linear load.

4.2 Methods to restrain inrush current and harmonic content

The following sections present the complete simulation model for each current limitation method. All methods were based on a common base model, see Section 4 above, enabling a reliable comparison and supporting the evaluation of which limitation method performs best.

4.2.1 Inrush reactor

Figure 4.4 illustrates a simplified version of the simulation setup using an inrush reactor. Measurements were still performed at points A-D as described in Section 4.1, illustrations and values from the simulation are presented in Section 5.2.1.

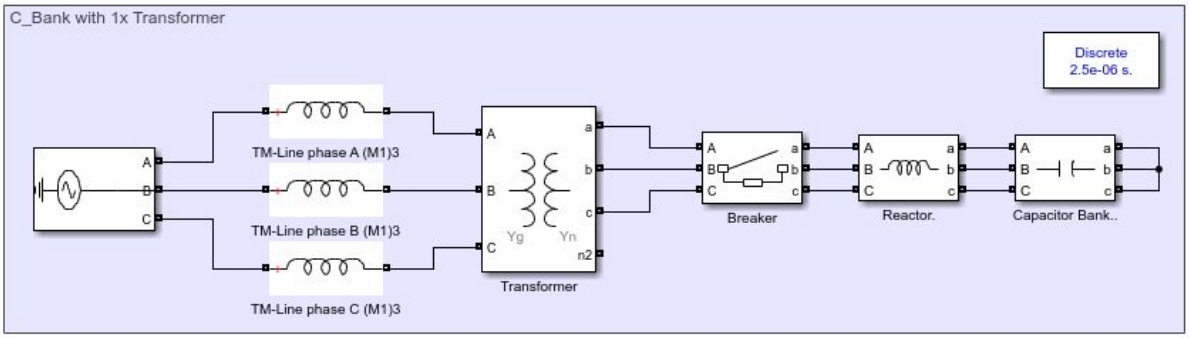

Figure 4.4: Complete model of series reactor limiting inrush current.

4.2.2 Pre-insertion resistor

Figure 4.5 illustrates the complete simulation model using a pre-insertion resistor. The breaker connected to the resistor closes first, allowing the capacitor to magnetize in a step, followed by the breaker connecting directly to the capacitor bank. Measurements are performed as described in Section 4, and corresponding figures and results are presented in Section 5.2.2.

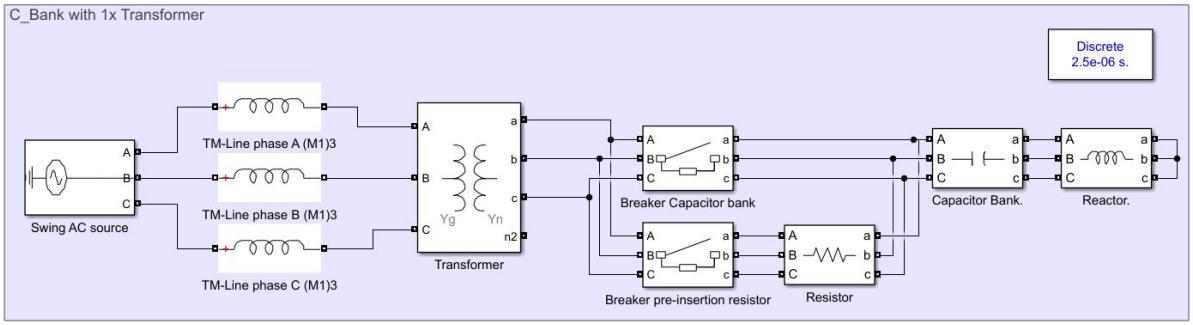

Figure 4.5: Complete model of inrush current limitation using a pre-insertion resistor, allowing a step magnetization of the capacitor bank.

Figure 4.6 illustrates a pre-insertion resistor similar to the one described above but with one major difference, a variable pre-insertion resistor. The variable resistor is electronically controlled with a linear function gradually decreasing the resistance to zero.

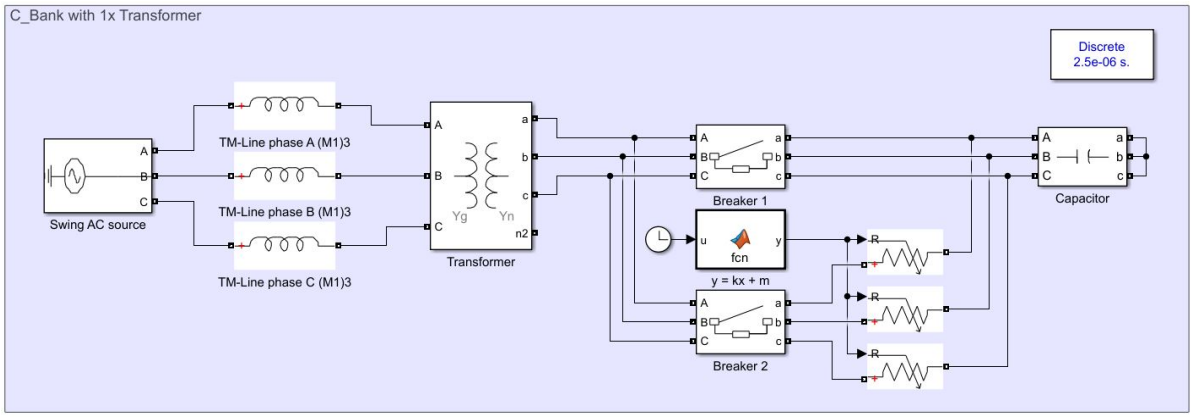

Figure 4.6: Complete model of inrush current limitation using a variable pre-insertion resistor, allowing a gradual magnetization of the capacitor bank.

4.2.3 De-tuned filter

To implement a de-tuned filter, the same configuration as illustrated in Figure 4.4 was used. However the size of the series reactor was calculated based on a desired tuning frequency between the resonance of the capacitor and the reactor. As mentioned in Section 3.3.3, two resonance frequency's where evaluated. Order 4th of fundamental (200Hz), and 4.7 of fundamental (235Hz).

4.2.4 Thyristor-switched capacitor

Figure 4.7 illustrates the complete model of a three phase TSC configuration. As described in 3.3.4 the thyristors conduct each phase separately to ensure $U_{C0} = U_{bus}$. Since Simulink does not allow to set an initial value of the three-phase capacitor block, the capacitor was exchanged for three separate single-phase capacitor blocks instead. Which allows for pre-charges values to be set.

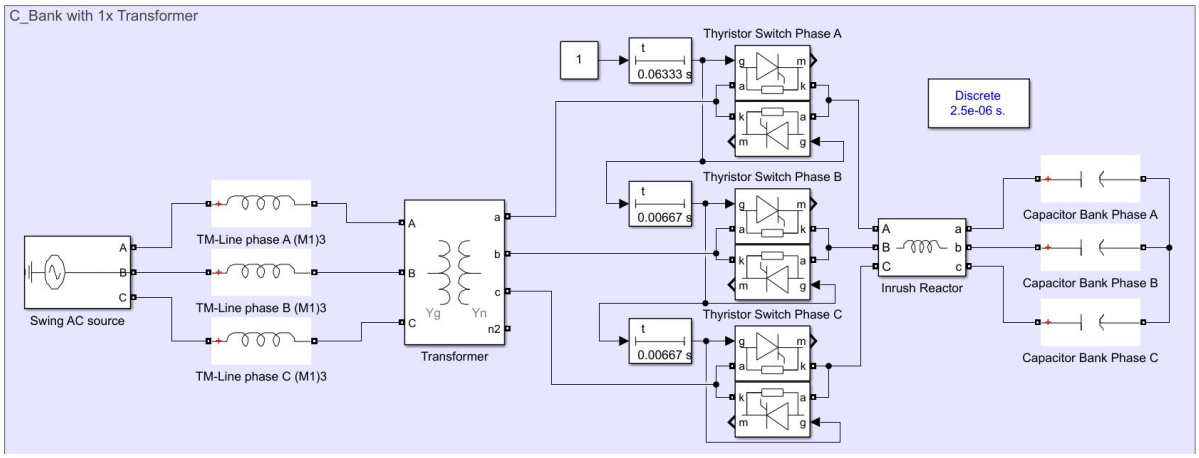

Figure 4.7: Complete model on a three phase TSC, allowing separate control of each phase.

5

Result

The following chapter presents the results from the simulations, including both the basic simulation model and the methods used to restrain inrush current. Furthermore, various factors influencing the magnitude of the inrush current and the harmonic content are clarified. The possibility to restrain or enhance harmonic content is also clarified for each method.

5.1 Connection of capacitor without current limitation at different grid impedance

Reminder: As explained in Section 4.1, voltage deviation refers to the excess voltage remaining after the fundamental oscillation has been subtracted from the main resulting waveform. Therefore neither 50Hz frequency or the main 1 p.u amplitude can be found in the voltage deviation graph. Only the deviating frequency and amplitudes are considered as a deviation.

It is clear that a stronger (low impeded) grid leads to smaller voltage deviations. As shown in Table 5.1, the voltage deviation exceeds 1 p.u. already at a compensation level of 4kVAr. In contrast, the stronger grid presented in Table 5.1 maintains the voltage deviation below 1 p.u. throughout the entire range. However, Table 5.1 also indicates a higher peak current, which is expected, as a stronger grid can supply current more rapidly, as discussed in Section 2.4.

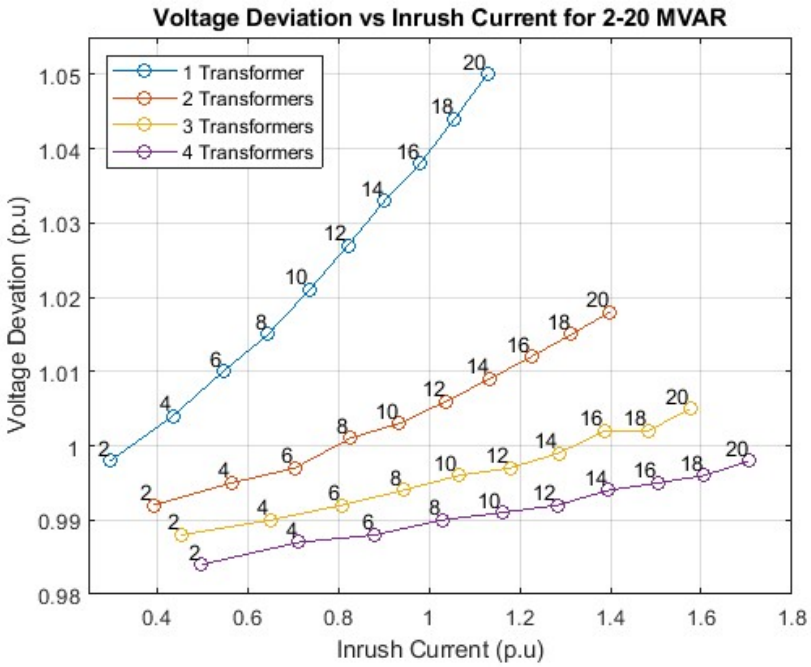

Figure 5.1: Relationship between inrush current and voltage deviation for capacitor banks of 2 to 20 MVAr, under different grid strengths. A stronger grid results in lower voltage deviation but larger current transients for the same compensation level.

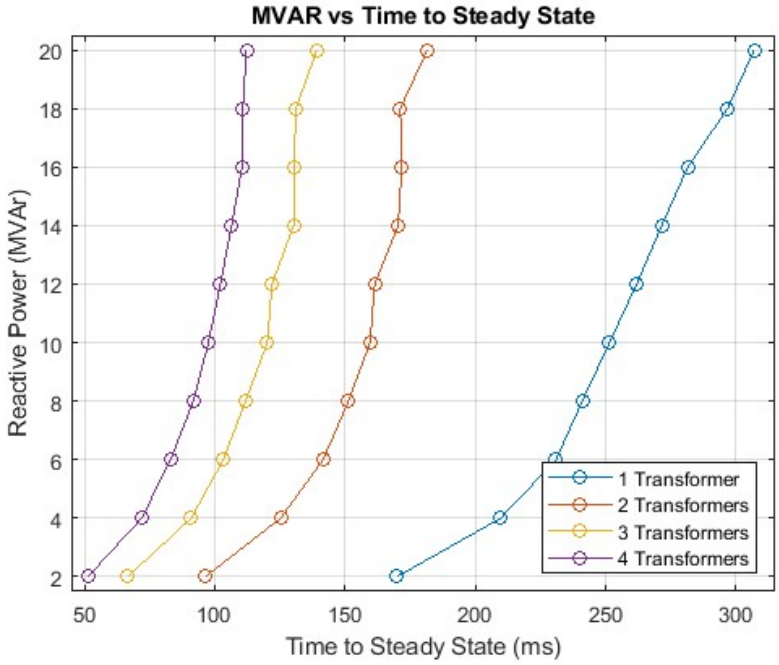

Figure 5.2: Time to steady state as a function of reactive power for different grid strengths. A stronger grid results in shorter stabilization times for the same compensation level. It can be seen in the graph that a grid consisting of 2 or 3 transformers significantly enhances the damping of oscillations in the system.

Table 5.1: Simulation results for different compensation levels for varying grid impedance

(a) Grid impedance based on one transformer.

Q (kVAr)	$\hat{U}$ (p.u.)	$\hat{I}$ (p.u.)	t (ms)
2	0.998	0.299	169.9
4	1.004	0.436	209.7
6	1.010	0.547	231.0
8	1.015	0.646	241.0
10	1.021	0.737	251.5
12	1.027	0.822	261.9
14	1.033	0.903	271.5
16	1.038	0.981	281.5
18	1.044	1.056	296.8
20	1.050	1.129	307.0

(b) Grid impedance based on two transformers.

Q (kVAr)	$\hat{U}$ (p.u.)	$\hat{I}$ (p.u.)	t (ms)
2	0.992	0.393	96.4
4	0.995	0.566	125.3
6	0.997	0.705	141.6
8	1.001	0.826	151.3
10	1.003	0.935	159.6
12	1.006	1.038	161.4
14	1.009	1.134	170.4
16	1.012	1.226	171.8
18	1.015	1.314	171.2
20	1.018	1.399	181.6

(c) Grid impedance based on three transformers.

Q (kVAr)	$\hat{U}$ (p.u.)	$\hat{I}$ (p.u.)	t (ms)
2	0.988	0.454	66.6
4	0.990	0.651	91.0
6	0.992	0.808	103.3
8	0.994	0.943	111.8
10	0.996	1.066	120.2
12	0.997	1.179	122.0
14	0.999	1.286	130.3
16	1.002	1.387	130.4
18	1.002	1.483	131.2
20	1.005	1.576	139.2

(d) Grid impedance based on four transformers.

Q (kVAr)	$\hat{U}$ (p.u.)	$\hat{I}$ (p.u.)	t (ms)
2	0.984	0.500	51.3
4	0.987	0.713	71.99
6	0.988	0.882	83.10
8	0.990	1.029	91.8
10	0.991	1.161	97.6
12	0.992	1.283	102.2
14	0.994	1.396	106.5
16	0.995	1.504	110.5
18	0.996	1.607	110.8
20	0.998	1.706	112.2

5.1.1 Harmonic content with non-linear load and no filter

Figure 5.3 illustrates the normalized FFT spectrum of the total system with a compensation of 8 MVAr. The amplitude of the fifth harmonic is 0.02 p.u. and 0.024 p.u. of the seventh harmonic. The resulting THD was 5.68%.

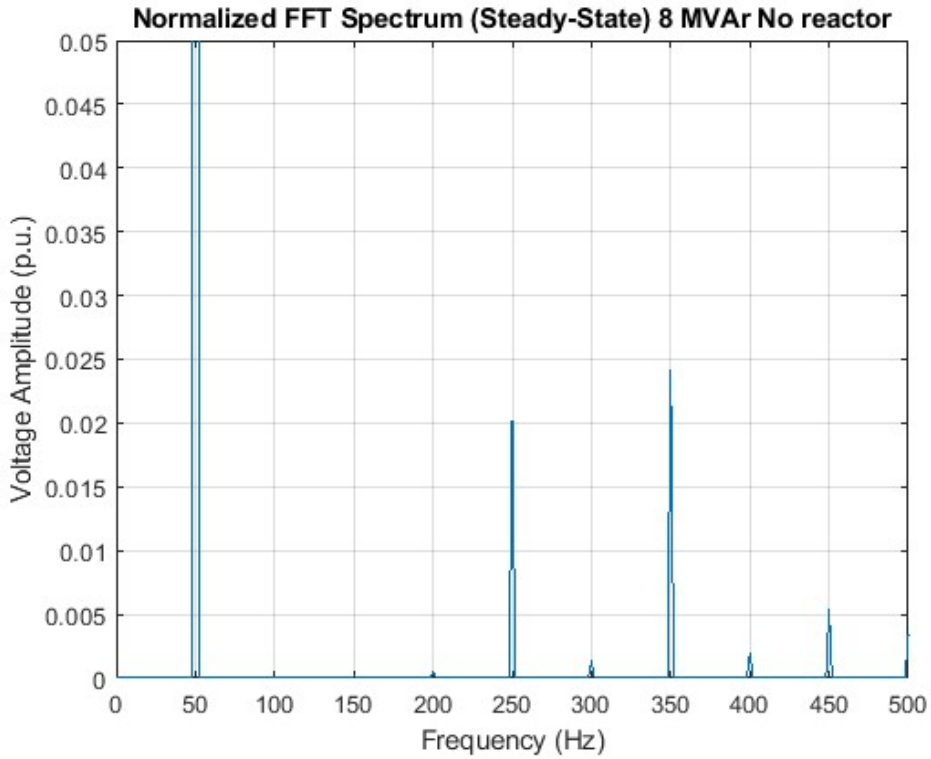

Figure 5.3: Frequency spectrum, no reactor, 8 MVAr.

By changing the amount of compensation, the amplitudes of both the 5th and 7th harmonics change to 0.028 p.u. and 0.055 p.u., respectively. This was expected, since the resonant frequency changes when either L or C in the system changes, according to Equation 2.9. The THD was 3.88

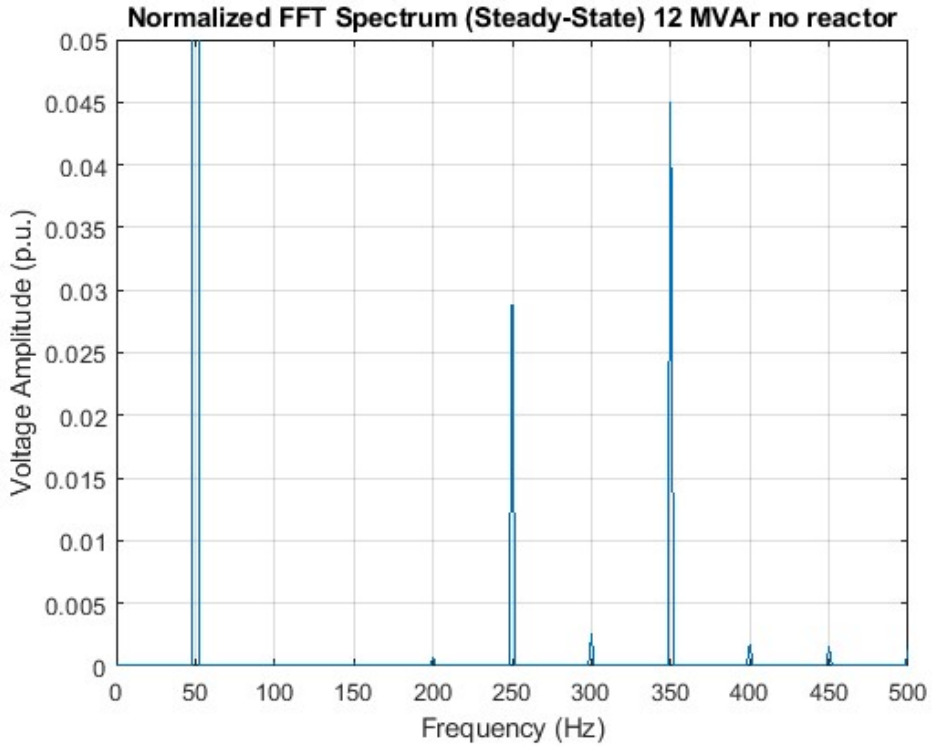

Figure 5.4: Frequency spectrum, no reactor, 12 MVAr.

5.2 Limitation methods

The following sections will present the results of each limitation method evaluated and if they fulfill or nor fulfill the requirements for class 1 in the IEC 61000-2-4 standard described in Section 3.1. The graphs are provided with a guiding reference line of ± 8% deviation. Which corresponds to the none-timely specified voltage deviation tolerance, relative to nominal voltage U_n [11]. Even though the result of the graphs are mainly evaluated in the scope of accepted transient deviation according to Figure 3.2, having the ± 8% lines of reference gives a better perception of the deviation scaling. Also a black line at 0.5 seconds help to understand the length of oscillations.

5.2.1 Inrush reactor

A normal sized inrush reactor of 100 µH results in a inrush current of 0.6182 p.u., a voltage deviation peak of 0.911 p.u. and it took 311 ms to reach steady state. The voltage deviations are shown in Figure 5.5. The tuning frequency is approximately 288 Hz, i.e. at the harmonic component 5.76, as can be ssen in Figure 5.6 neither of the 5th or 7th harmonic were suppressed. The size of this reactor does not fulfill the demand of the standard.

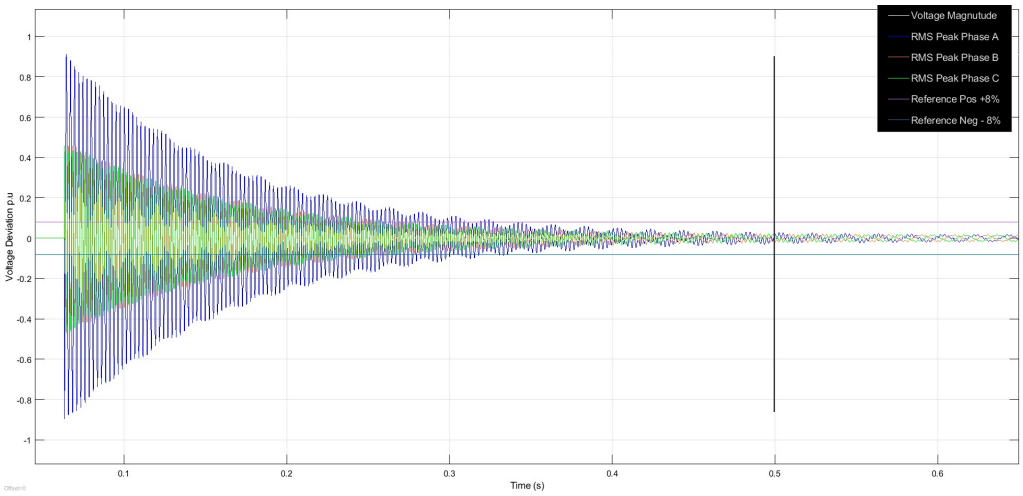

Figure 5.5: Voltage deviation when a 100 uH reactor is used.

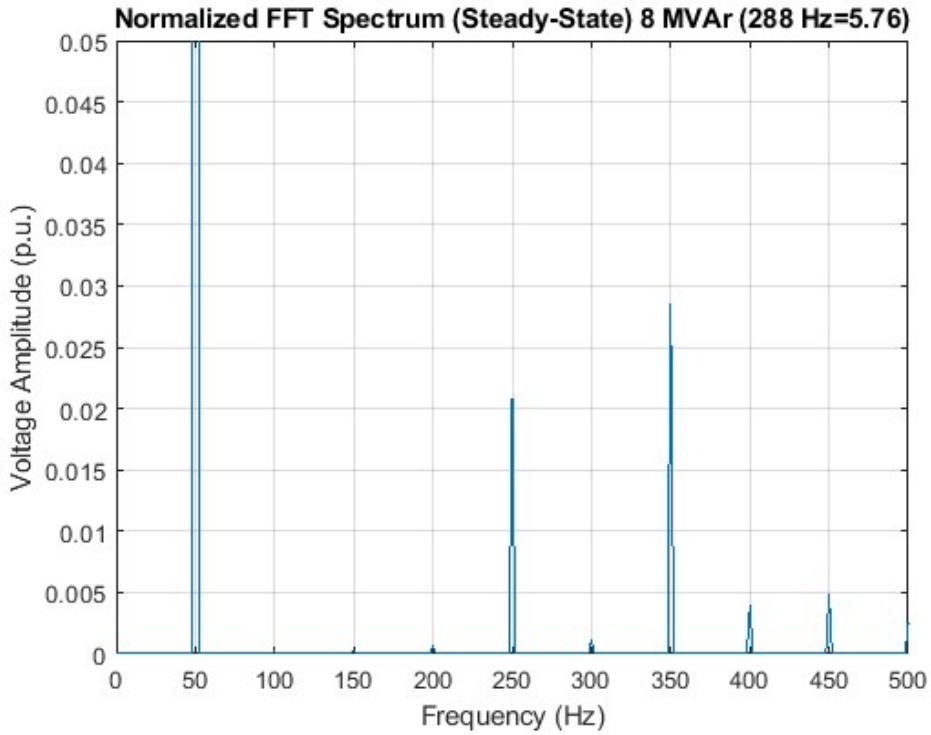

Figure 5.6: Frequency spectrum with a 100 uH inrush reactor.

To stay within the requirements of the standard, the inrush reactor had to be of a size of at least 4 mH. This inductance results in a inrush current of 0.348 p.u., a voltage peak of 0.1993 p.u. and 660 ms to reach steady state. Results of the simulated voltage deviation is illustrated by Figure 5.7. The tuning frequency for this reactor size was 173 Hz, i.e. at harmonic component 3.46. The normalized FFT spectrum is shown in Figure 5.8 where the 5th harmonic had an amplitude of 0.007 p.u. and a THD of 4.99% and thereby fulfilled the requirements for Class 1 regarding harmonic content.

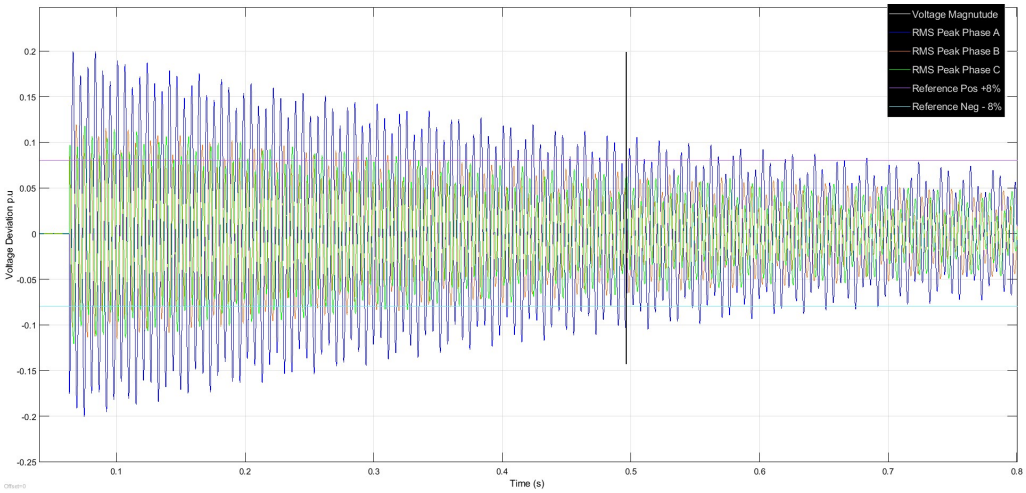

Figure 5.7: Voltage deviation when a 4 mH inductor is used.

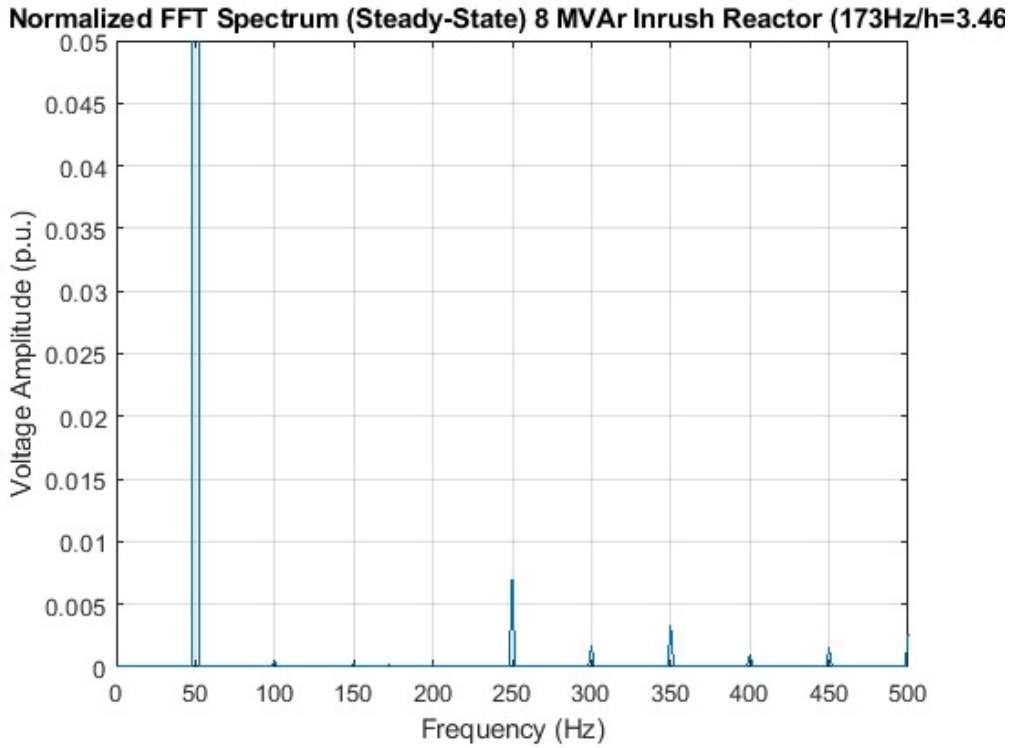

Figure 5.8: Frequency spectrum with a 4 mH inrush reactor.

5.2.2 Pre-insertion resistor

Since the breaker to the capacitor bank was closed before the breaker to the pre-insertion resistor was opened, the capacitor bank was connected at a point where the voltage magnitude of each phase corresponds to the voltage magnitude of the bus/grid, mitigating inrush current and voltage deviation successfully. The method fulfills the requirement for class 1 in the standard as it resulted in an initial voltage peak of 0.878 p.u. for t =335.833 µs and a current peak of 0.231 p.u. when the

pre-insertion resistor was connected. The inrush current of the second peak was 0.195 p.u., with a voltage peak of 0.2 p.u. for $t = 85.527ms$ and it took $t = 102ms$ to reach steady state. Figure 5.9 illustrates the result of the simulation.

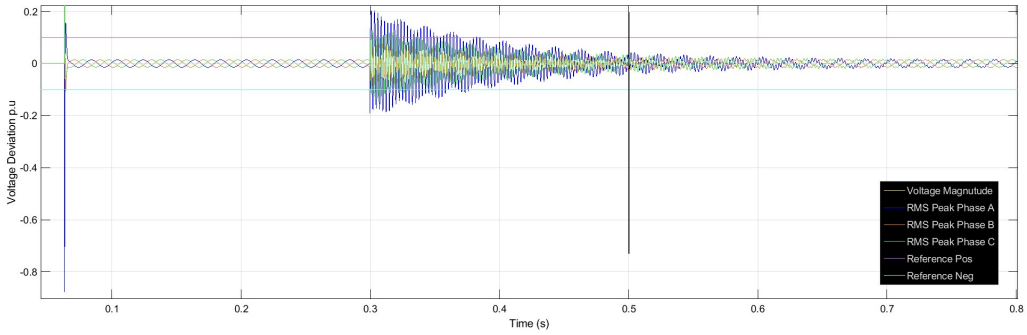

Figure 5.9: Voltage deviation when a 4 Ω pre-insertion resistor was used.

A variable pre-insertion resistor results in almost no volta fluctuation as can be seen in Figure 5.10. There is an initial voltage transient of 0.73 p.u. with a very short duration and thereby without doubt fulfills the requirements for Class 1 in the standard. However, neither of these two cases provides any sort of filtering effect.

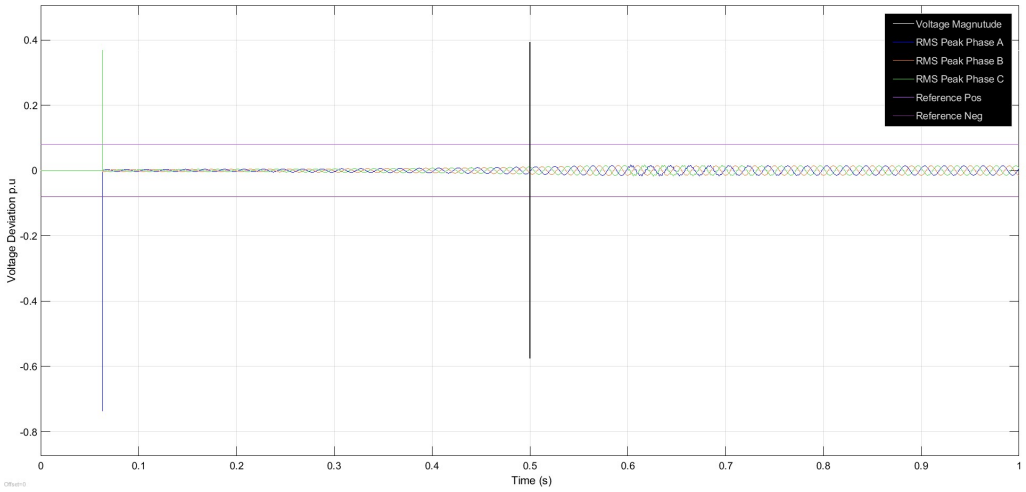

Figure 5.10: Voltage deviation when a variable 100 Ω-0 Ω pre-insertion resistor was used.

5.2.3 De-tuned filter

Case 1, described in Section 3.3.3, have a tuning frequency of 235 Hz and resulted in an inrush current of 0.424 p.u., a voltage peak of 0.345 p.u., and the time to steady state was 536 ms. As can be seen in Figure 5.11, illustrating the voltage deviation for Case 1, it does not fulfill class 1 in the standard. The normalized FFT spectrum is shown in Figure 5.12, the amplitude of the 5th harmonic was 0.019 p.u., and the THD for Case 1 was 5.13%, which does not fulfill the THD requirements for Class 1.

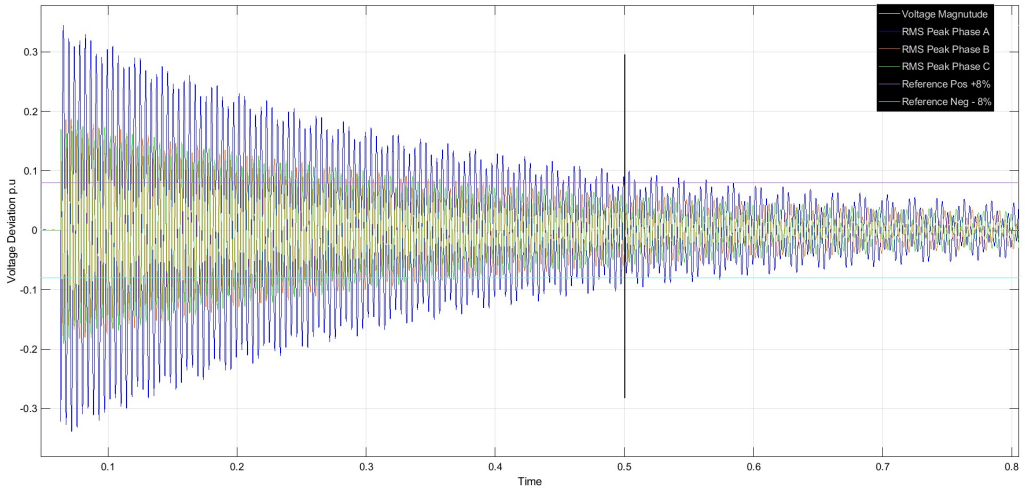

Figure 5.11: Voltage deviation when a filter reactor of 1.793 mH was used.

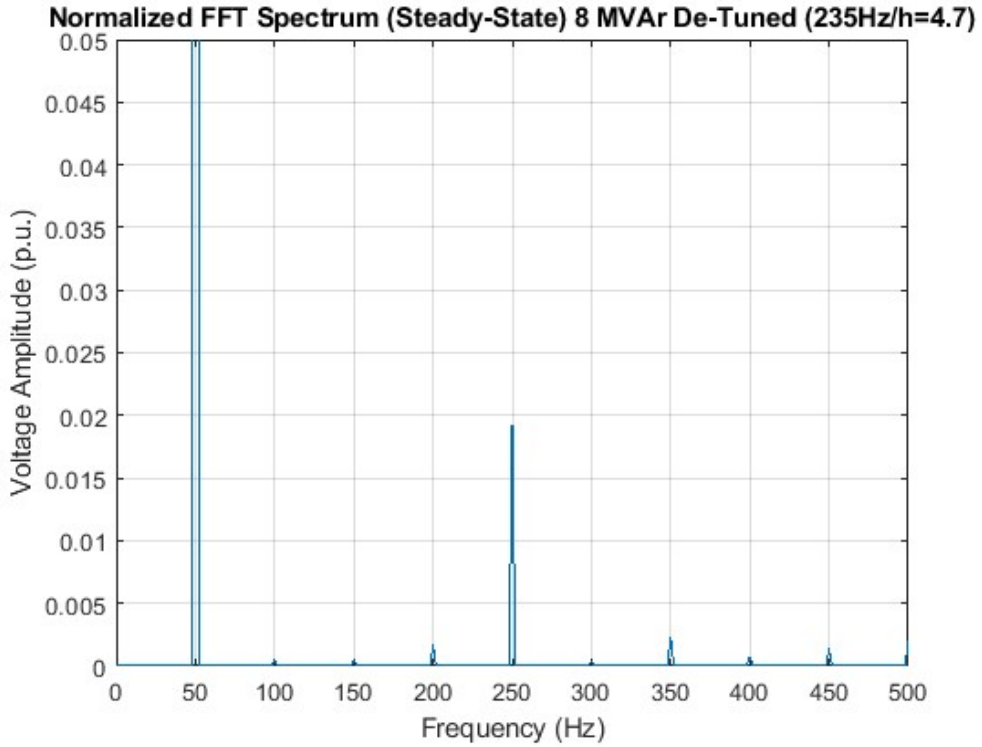

Figure 5.12: Frequency spectrum of tuning frequency 235 Hz.

Case 2 had a tuning frequency of 200 Hz and resulted in an inrush current of 0.385 p.u., a voltage peak of 0.264 p.u., and the time to steady state was 590 ms. Figure 5.13 shows the voltage deviation and that the strategy does not fulfill the demand for class 1 in the standard. The normalized FFT spectrum for Case 2 is shown in Figure 5.14, the 5th harmonic had an amplitude of 0.0049 p.u. and the THD for Case 2 was 4.97%, and is within the accepted level of THD for Class 1..

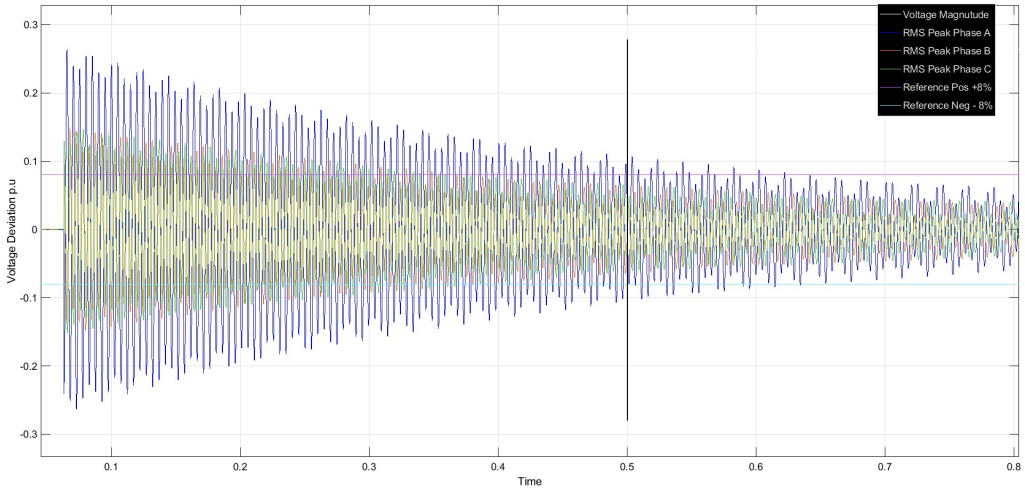

Figure 5.13: Voltage deviation when a filter reactor of 2.687 mH was used.

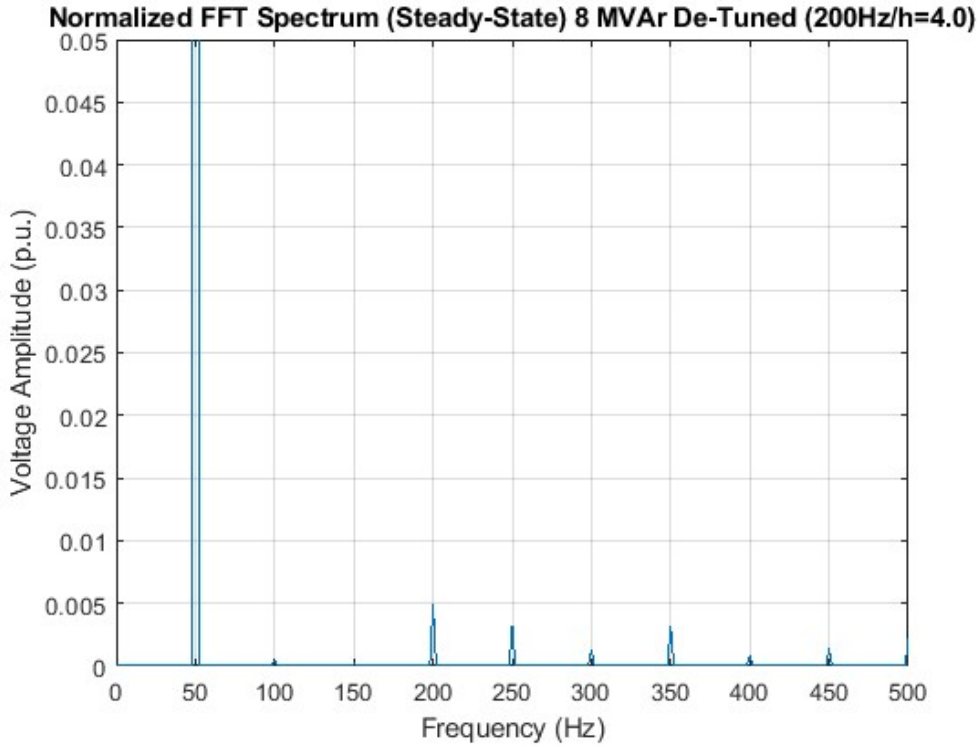

Figure 5.14: Frequency spectrum of tuning frequency 200 Hz.

5.2.4 Thyristor-switched capacitor

As can be seen in Figure 5.15, and cross referenced with the single phase example in Section 2.4, switching the initial phase A when U_{C0}=U_{bus} allows for almost transient free switching. When conducting phase B and C, transients and oscillations occur in a similar manner as previous methods. Extending the interval between conducting each phase, as in Case 2, did not improve the transient peaks or time to steady state, see Figure 5.16. The voltage peak reached 0.798 p.u., the current transient peak

reached 0.591 p.u. and time to steady state was 454 ms for Case 1. When analyzing the harmonic content of the thyristor switching mechanism, almost no additional switching harmonics is introduced in the FFT spectrum and the THD remained very low at 0.01%. This indicates that the thyristors continuous switching during steady state operation is not a source of harmonic distortions in the system. Other then the small inrush reactor there is no filtering effect provided by this method. Consequently the method does not fulfill the requirements for Class 1 in the standard when switching att medium voltage levels.

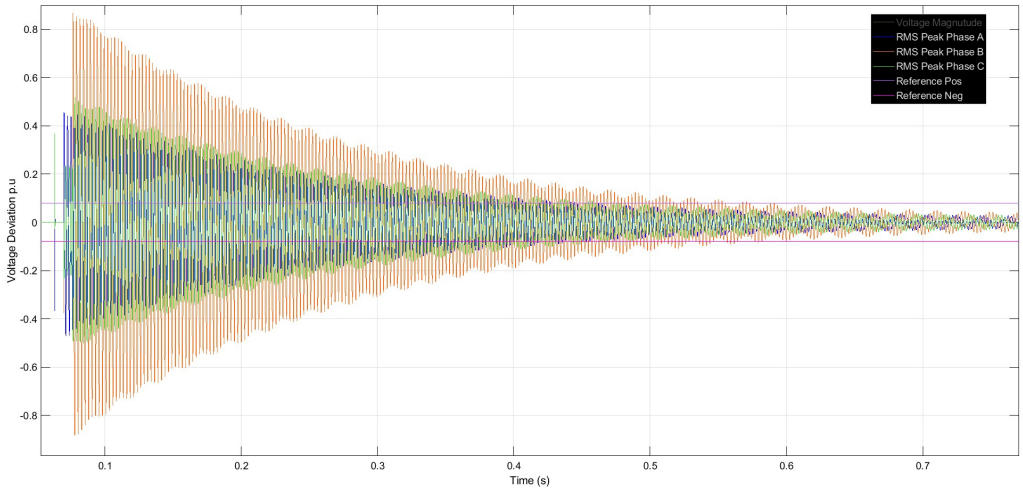

Figure 5.15: Voltage deviation of a TSC, Case 1.

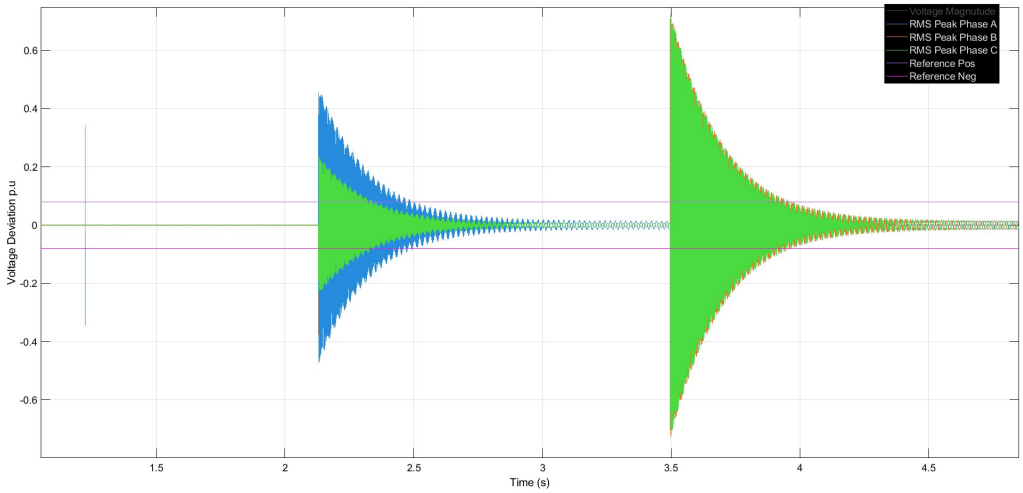

Figure 5.16: Voltage deviation of a TSC, Case 2.

6
Conclusions and discussion

When selecting a current inrush limitation method, there are many aspects to consider. Even though some of these methods may achieve similar results in regards to limiting the inrush currents, their characteristics make them applicable in different cases. The most predominant parameter to establish before selecting a limitation method is the accepted transient levels of the equipment on site. Also, what level reactive compensation is needed or if the need of filtering is greater than the need of compensation.

The normal inrush reactor as covered by Section 2.5.1 generally found as a part of the capacitor bank by default, does not provide any substantial limitation of inrush current, and could rather be referred to as a method of disaster management, offering only minimal mitigation in the event of faults or similar disturbances in the grid. It cannot be recommended as a default solution for safely connecting a capacitor bank to the grid alone.

To achieve a better limitation effect, a larger inductance is required. Increasing the inductance will dampen the inrush current more, and thereby the voltage fluctuations will be less. Increasing the size of the inrush reactor enough, or respectively to a specific value could potentially have the reactor serve two proposes simultaneously. Namely, provide a filtering effect in combination with current limiting properties. As can be seen in the simulation: A reactor sized in a fashion to purely represent an inrush reactor, will be large enough to interact with the dangerous harmonics of the system. Also, it is about the same size as a reactor included in a de-tuned filter. A large reactor setup in configuration as a de-tuned filter, could offer an elegant way of solving two issues of filtering and limitation in an industrial facility. The de-tuned filter with a tuning frequency of 200 Hz preformed better in suppressing harmonics then the de-tuned filter tuned to 235 Hz. This could be an affect of the 235 Hz being to close to the 5th harmonic and therefor not suppressing it the 5th harmonic enough.

However, increasing the reactor size comes at a cost. An increase in L will also make the resulting amount of Q compensation provided by the capacitor bank to be less. It is therefore not possible to only consider acceptable transient magnitudes when selecting a limitation method involving a reactor, since this is heavily dependent on the amount of Q compensation required at the facility. The de-tuned filter solution will therefore have to be dimensioned in co-ordinance of the resonating harmonic frequency's of the respective facility, and then scaled up to matched the need of capacitive Q compensation relative to it's $cos\varphi$ angle. As mentioned earlier,

see Section 1.1, this might not be an issue for modern Swedish industries after all. Since most industries are replacing older, mainly inductive, electrical machines with drive system-controlled solutions, the need of reactive power compensation is therefor decreasing. That is why it could be considered acceptable that the amount of Q compensating power reduces with reactor size. It is however important to consider that an increase of L significantly increase the physical size of the reactor, according to Equation 2.8. If space is a limitation, this solution would not be feasible due to it´s potentially massive size and weight. A lower tuning frequency requires a larger reactor, equivalently a larger L.

The pre-insertion resistor solution is the most space effective solution in terms of size. However, it does require two breakers to operate in it's most basic form. If also paired with a larger standard inrush-reactor, meaning a reactor that is far less of size to serve with a filtering effect, but just a bit larger than the regular standard inrush-reactor, this solution could potentially stay well within the limits of the Class 1 voltage quality. Making it a viable option even for very sensitive equipment scenarios, while not requiring a reactor of very large size and weight. In terms of efficiency and ease of deployment, this is likely the most effective approach of connection.

Since the pre-insertion resistor main issue is that it changes the resistance in discrete steps, and not posing a smooth transition in terms of connecting the capacitor bank, the approach explored with variable resistance pre-insertion resistor solves this issue. In simulation, this could provide an almost entirely transient free connection, with no introduction of any switching harmonics before steady state what so ever. This, paired with a regular small inrush-reactor is by far the best solution in theory and could be explored further since variable resistors exist on market for other forms of application. If deployed correctly, this could also eliminate the need of an extra breaker which would assist in the reduction of additional complexity.

A modern approach to limit transients in switching strategy is implementation of TSC, usually considered a part of the SVC. Assuming that the basic theory in Section 2.5.4 is used to achieve the same voltage levels while switching, an almost transient free switching could be achieved. This was the case for single phase, as shown in the example provided in Section 2.4, however, large transients occurred in the three phase system, as the capacitor bank has a common ungrounded neutral point connected to each other, thus creating a voltage potential in between phases due to the time lag during connection while phase B and C are waiting to be connected. Due to the limited time scope of this project, we were unable to investigate the optimal connection timing in the TSC. To the best of our understanding, the inrush current could potentially be further reduced by adjusting the connection timing to minimize the voltage differences between the charged capacitors, the capacitor bank, and the bus voltage. However, a perfect result is still not achievable. TSC can therefore not be considered as a method of transient free switching in three phase systems which is a general misconception. It does however significantly reduce the amount of transient that are happening compared to a random synchronous switched con-

nections. TSC is more effective in terms of transient impact, when deployed at lower voltage or with smaller banks in steps. If varying load angle is an issue on site, with requirements of fast load angle management. For example, electric machines at an industry that starts and stops very frequently, is a root source of changing load angle characteristic and could benefit from a TSC controlled capacitor bank. But due to the large size of the capacitor bank analyzed, which purpose is to provide reactive power compensation for all/many machines/equipment. It is not reasonable to make the assessment that very large industry wide capacitor banks needs to be connected and disconnected for real-time management purposes. It makes more sense to handle this at lower voltage levels closer to the equipment requiring the compensation.

It should also be mentioned that the nominal power of the transformer affects the results in different ways. Section 3.2.2 discusses this issue and that the transformer could be considered over dimensioned for this application. The use of a transformer with lower nominal power would affect the result since the total impedance of the transformer increases and therefore the inrush current transient would decrease, meanwhile the voltage fluctuations would increase due to the effect of a weaker grid, as discussed in Section 2.4. This reasoning could be strengthened by simulation results in Section 5.1. A higher rated transformer is similar to four parallel transformer, representing a stronger grid and a lower rated transformer is similar to the case of one transformer, representing a weaker grid with higher impedance. Changing the rated power of the transformer would also affect the resonant frequency of the total system, an increase of internal inductance would create a lower resonant frequency, if all other parameters are assumed to remain unchanged.
The use of a different simulation software could also possible enhance precision of the outcome. While MATLAB is able to perform transient analysis, there are more acknowledged simulation software available with enhanced models of the components that was used. Power Factory is one example of this that is more used by the scientific community and power engineering companies for transient analysis. But since this report aims to provide a basic understanding of the different switching methods by primarily changing certain components in a fixed system design and logging a response in a broader scope, MATLAB was considered accurate enough. If a specific site analysis is to be performed for installing certain equipment on site. Simulations in a software like Power Factory could be something to consider due to more precise modeling of components and better solver settings.

In general: Facilities in need of mainly Q compensation and not requiring filtering affect, a pre-insertion solution is recommended since it maximizes the Q compensation and is easily implementable. A facility in need of filtering effect and less Q compensation should implement a combination of pre-insertion resistor along with a de-tuned filter or a small inrush reactor, dependent on the system total inductance, to limit the inrush current enough and suppress a chosen range of frequency's.

Bibliography

[1] Western Area Power Administration, "Mead substation capacitor bank," *Flickr*, Apr. 2014. [Online]. Available: https://www.flickr.com/photos/westernareapower/14030580366

[2] P. Mphahlele, B. Mendu, and B. B. Monchusi, "Exploring of Power System Methods on Power Factor Improvement and Reactive Power Compensation," in *International Conference on Electrical, Computer and Energy Technologies (ICECET)*, Cape Town, South Africa, Nov. 2023, pp. 1-10. [Online]. Available: https://doi.org/10.1109/ICECET58911.2023.10389347. Accessed: 2025-03-21.

[3] S. Suresh, R. Gnanadass and N. P. Subramaniam, "Design and analysis of a cost effective power quality improvement method using De-tuned filter," in *IEEE International Conference on Electrical, Instrumentation and Communication Engineering (ICEICE)*, Karur, Indien, Apr. 2017, pp. 1–7. [Online]. Available: https://doi.org/10.1109/ICEICE.2017.8191956, Accessed: 2025-04-11.

[4] M. F. McGranaghan and D. R. Mueller, "Designing harmonic filters for adjustable-speed drives to comply with IEEE-519 harmonic limits," IEEE Transactions on Industry Applications, vol. 35, no. 2, pp. 312–318, Apr. 1999, doi:10.1109/28.753622.

[5] A. Zhai, Y. Fan, Z. Li, and M. Gao, "Study on the Analysis and Suppression Methods of Inrush Current in Power Capacitor Switching," in *IEEE 4th International Conference on Information Technology, Big Data and Artificial Intelligence (ICIBA)*, Chongqing, China, Dec. 2024, pp. 517–521. [Online]. Available: https://doi.org/10.1109/ICIBA62489.2024.10868178, Accessed: 2025-03-21.

[6] M. Bongiorno, "Lecture 7: Shunt-connected FACTS – TSC and SVC," unpublished.

[7] N. Gothelf, private communication, Apr. 2025.

[8] Z. Popović and B. Popović, *Introductory Electromagnetics*. 1st ed., Upper Saddle River, New Jersey, USA: Prentice Hall, 2000.

[9] S. Katyara, A. A. Hashmani, and B. S. Chowdhry, "Analysis and Mitigation of Shunt Capacitor Bank Switching Transients on 132 kV Grid Station, Qasimabad Hyderabad," in *Mehran University Research Journal of Engineering and Technology*, Pakistan, Jul. 2015, vol. 34, no. 3, pp. 291–300. [Online]. Available: https://research.ebsco.com/linkprocessor/plink?id=33d3a743-3277-347f-b6c0-9ece5294df8a

[10] F. Ma, C. He, X. Chen, X. Zhu, J. Deng, and H. Ni, "Suppression Methods of 750 kV AC Filter Switching Inrush Surge for Circuit Breakers Having Pre-

insertion Resistors," in 4th International Conference on HVDC (HVDC), Xi'an, China, Nov. 2020, pp. 1207-1212. [Online]. Available: https://doi.org/10.1109/HVDC50696.2020.9292746, Accessed: 2025-03-21.

[11] Electromagnetic compatibility (EMC) – Part 2-4: Environment – Compatibility levels in power distribution systems in industrial locations for low-frequency conducted disturbances, IEC 61000-2-4, International Electrotechnical Commission, Geneva, Switzerland, 2024. Available: https://www-sis-se.eu1.proxy.openathens.net/api/document/get/82089563

[12] MathWorks, "Three-Phase Source," 2024. [Online]. Available: https://se.mathworks.com/help/sps/powersys/ref/threephasesource.html (Accessed: 2025-03-25).

[13] MathWorks, "Three-Phase Transformer," 2024. [Online]. Available: https://se.mathworks.com/help/sps/powersys/ref/threephasetransformertwowindings.html (Accessed: 2025-03-25).

[14] MathWorks, "Three-Phase Series RLC Branch," 2024. [Online]. Available: https://se.mathworks.com/help/sps/powersys/ref/threephaseseriesrlcbranch.html (Accessed: 2025-03-25).

[15] MathWorks, "C Function," 2024. [Online]. Available: https://se.mathworks.com/help/simulink/slref/cfunction.html (Accessed: 2025-03-25).

A

Appendix 1

A.1 Source code listing

Listing A.1: MATLAB code to find time to steady state.

```
\begin{lstlisting}[frame=single]
/* Includes_BEGIN */
#include <math.h>
#define THRESHOLD 0.1  // 10% threshold
#define HOLD_TIME 500
/* Includes_END */

/* Externs_BEGIN */
/* extern double func(double a); */
static double peak_u0 = 0.0;
static double peak_u1 = 0.0;
static double peak_u2 = 0.0;
static int stable_count = 0;
static double time_keeper = 0.0;
/* Externs_END */

void trig_Start_wrapper(void)
{
/* Start_BEGIN */
/*
 * Custom Start code goes here.
 */
    peak_u0 = 0.0;
    peak_u1 = 0.0;
    peak_u2 = 0.0;
    stable_count = 0;
    time_keeper = 0.0;
/* Start_END */
}

void trig_Outputs_wrapper(const real_T *u0,
                          const real_T *u1,
                          real_T *y0,
                          real_T *y1)
{
```

```
/* Output_BEGIN */
// Update peak values dynamically
    if (fabs(u0[0]) > peak_u0) peak_u0 = fabs(u0[0]);
    if (fabs(u0[1]) > peak_u1) peak_u1 = fabs(u0[1]);
    if (fabs(u0[2]) > peak_u2) peak_u2 = fabs(u0[2]);

    // Compute threshold limits
    double limit0 = peak_u0 * THRESHOLD;
    double limit1 = peak_u1 * THRESHOLD;
    double limit2 = peak_u2 * THRESHOLD;

    // Check if all signals are within their respective
    thresholds
    if (fabs(u0[0]) < limit0 && fabs(u0[1])
    < limit1 && fabs(u0[2]) < limit2) {
        stable_count++;
    } else {
        stable_count = 0;  // Reset if any signal goes above the
        threshold
    }

    // Set output when stability is maintained for HOLD_TIME
    iterations
    if (stable_count >= HOLD_TIME) {
        y0[0] = 1.0;
        y1[0] = time_keeper;
        //time_keeper = time_keeper;
    } else {
        y0[0] = 0.0;
        time_keeper = u1[0];
    }
/* Output_END */
}

void trig_Terminate_wrapper(void)
{
/* Terminate_BEGIN */
/*
 * Custom Terminate code goes here.
 */
/* Terminate_END */
}
```

Listing A.2: MATLAB code to find peak voltages

```
/* Includes_BEGIN */
#include <math.h>
/* Includes_END */

/* Externs_BEGIN */
```

```
/* extern double func(double a); */
static double phase_A;
static double phase_B;
static double phase_C;
double max;
/* Externs_END */

void peak_catcher_Start_wrapper(void)
{
/* Start_BEGIN */
max = 0;
/* Start_END */
}

void peak_catcher_Outputs_wrapper(const real_T *u0,
                                  real_T *y0)
{
/* Output_BEGIN */
phase_A = u0[0];
phase_B = u0[1];
phase_C = u0[2];


    if(phase_A > max){
        max = phase_A;
    }else if(phase_B > max){
        max = phase_B;
    }else if(phase_C > max){
        max = phase_C;
    }else{
        y0[0] = max;
    }
/* Output_END */
}

void peak_catcher_Terminate_wrapper(void)
{
/* Terminate_BEGIN */
/*
 * Custom Terminate code goes here.
 */
/* Terminate_END */
}
```

Listing A.3: MATLAB code to find peak currents

```

/* Includes_BEGIN */
#include <math.h>
/* Includes_END */
```

```
5
6  /* Externs_BEGIN */
7  /* extern double func(double a); */
8  static double phase_A_current;
9  static double phase_B_current;
10 static double phase_C_current;
11 double max_current;
12 /* Externs_END */
13
14 void peak_current_catcher_Start_wrapper(void)
15 {
16 /* Start_BEGIN */
17 max_current = 0;
18 /* Start_END */
19 }
20
21 void peak_current_catcher_Outputs_wrapper(const real_T *u0,
22                                           real_T *y0)
23 {
24 /* Output_BEGIN */
25 phase_A_current = u0[0];
26 phase_B_current = u0[1];
27 phase_C_current = u0[2];
28
29
30     if(phase_A_current > max_current){
31         max_current = phase_A_current;
32     }else if(phase_B_current > max_current){
33         max_current = phase_B_current;
34     }else if(phase_C_current > max_current){
35         max_current = phase_C_current;
36     }else{
37         y0[0] = max_current;
38     }
39 /* Output_END */
40 }
41
42 void peak_current_catcher_Terminate_wrapper(void)
43 {
44 /* Terminate_BEGIN */
45 /*
46  * Custom Terminate code goes here.
47  */
48 /* Terminate_END */
49 }
```

Department of Electrical Engineering
CHALMERS TEKNISKA HÖGSKOLA
Gothenburg, Sweden
www.chalmers.se

CHALMERS